Climate Change Impact Assessment on Low Streamflows Using Cross-Entropy Methods in Iran's Namak Lake Basin

Zahra Sheikh[1]; Alireza Moghaddam Nia[2*]; Dawei Han[3]

[1] Department of Combat Desertification, Faculty of Desert Studies, Semnan University, 9861413615, Semnan, Iran

Email: (z.sheikh03@gmail.com) ;

[2] Department of Rehabilitation of Arid and Mountainous Regions, Faculty of Natural Resources, University of Tehran, 3158777871, Karaj, Iran ;

* Corresponding Author Email: (a.moghadamnia@ut.ac.ir)

[3] Department of Civil Engineering, University of Bristol, Bristol, BS8 1TR, UK

Email: (d.han@bristol.ac.uk)

A Short Title: Analysis of climate change by Cross-Entropy

Abstract

Climate change impacts on low streamflows provide a comprehensive picture of the state of surface and groundwater resources, particularly in arid and semi-arid regions. The objective of this study is to assess the impacts of climate change on low streamflow variations by detecting long-term spatiotemporal changes in recorded climatic variables such as rainfall and temperature, as well as their associations with low streamflow fluctuations. Seasonal variations in low streamflows (summer and winter) are examined at 18 hydrometric stations located in the Namak Lake Basin, Iran, between 1970 and 2015, using the nonparametric Modified-Mann-Kendall test and Sen's Slope Estimator method. Seasonal low streamflow has demonstrated a clear diminishing significant trend (in more than 55% of the stations), while summer low streamflow has showed a more pronounced and drastic decreasing trend (at 82% significance at a $p<0.01$ probability level). Long-term changes in boreal seasonal and annual rainfall/temperature also reveal a dominant decreasing trend in winter and spring rainfall (in 82% and 58% of all stations, respectively) and a dominant increasing trend in all temperature time scales (in 90% of all stations). The effects of climate variations on low streamflow are quantified by applying Spearman's rank correlation and Cross-SampEn methods. The results reveal that the winter rainfall, annual and summer temperatures have the strongest association with seasonal low streamflows, especially in the entropy method. Although the relationships between low streamflows and temperature/rainfall are related to the different processes that generate streamflows, particularly in heterogeneous locations, the results indicate that rainfall has a stronger influence on low streamflows in this region than temperature does. In addition, the findings of the research indicate that low streamflows are more nonlinearly related to climatic parameters like temperature and rainfall, and the robustness of Cross-SampEn reflects the degree of asynchrony for complex, non-linear, and non-stationary time series.

Keywords: Climate Change; Seasonal Low Streamflows; Association; Cross-SampEn; Namak Lake Basin

1. Introduction

Climate change is a worldwide challenge that has widespread implications for the hydrological cycle (Jehanzaib et al. 2020). An increase in the frequency, intensity, and duration of extreme events is one of the widely known consequences of climate change (Vlach et al. 2020). Currently, due to the extensive consequences of water scarcity resulting from extreme events (Wang et al. 2020), low streamflows and droughts are more and more identified as hazard situations (Cammalleri et al. 2017, Jehanzaib et al. 2020).

Low streamflow, known as the lowest section of the continuous streamflow hydrograph, is a yearly seasonal phenomenon (Dudley et al. 2020). Knowledge of the low streamflow variations and dynamics is essential for water quality and quantity management and riverine ecosystem protection (Konapala et al. 2018, Sheikh et al. 2020, Dudley et al. 2020). Additionally, as an essential component of the streamflow regime, low streamflow is a multi-dimensional component of streamflow that reflects the impacts of climate change and human intervention over time (Dudley et al. 2020).

According to reports and evidence of observed climate variations worldwide, identification, determination, and accounting of trends in low streamflow and their relationship with climate change can improve the current and future of low streamflow estimations, especially in arid regions. In addition, assessing trends and climatic associations enables knowledge and awareness of other driving forces of low streamflow variations (natural/anthropogenic factors). Assessment of long-term trends of low streamflows has been addressed in previous studies (Ali et al. 2019, Kuriqi et al. 2020, Tomaszewski & Kubiak-Wójcicka 2021). A growing number of studies have recently been focused on investigating low streamflow responses to climate change (Marx et al. 2018, Mahmoodi et al. 2020, Ghafouri-Azar et al. 2021). Several studies were conducted to look into the future of low streamflow variations estimations under various climate change scenarios (Foulon et al. 2018, Fangmann & Haberlandt 2019, Jehanzaib et al. 2020). Another research examined the long-term historical trends of observed hydro-climatic factors and discovered probable connections between low streamflows and climatic variables to determine the influence of climate change on low streamflows (Degefu & Bewket 2017, Konapala et al. 2018, Dudley et al. 2020). The typical approach of such research is using a simple correlation such as parametric and non-parametric methods such as Pearson and Spearman correlation coefficients to estimate the relationship between low streamflows and climate indices (Assani et al. 2011, Giuntoli et al. 2013, Degefu & Bewket 2017).

Currently, spectral analysis based on wavelet transform is being used as an efficient method to investigate the relationship between climate indices and low streamflows (Ling et al. 2013, Konapala et al. 2018). Although wavelet transform methods performed more favorable results than the linear correlation (Konapala et al. 2018), it should be considered that hydro-climatic systems are non-linear complex dynamic systems as a consequence of interactions among the atmosphere, hydrosphere, and geosphere (Lee et al. 2017). Streamflow fluctuations appear to indicate a complicated response to climate change (Shen et al. 2018). Based on the opinions of non-linear dynamic investigations and chaos, the standard statistics such as spectral and coherency measures are not appropriate for non-linear and non-stationary time series. As a result, a robust approach is required to analyze hydro-climatic variables' relationships with non-linear and non-stationary patterns.

Shannon (1948) originated the concept of entropy as the measure of information formulated based on the second law of thermodynamics. Shannon's entropy is a crucial measure of uncertainty, complexity, dispersion, diversification, or disorder of a variable. It can be considered as the negative expected content of the logarithm of a probability density function for the variable (Shannon 1948). Singh (2011), Liu et al. (2013), and Chou (2014) have provided comprehensive reviews of the entropyconcept and its application to hydrology and water resources, variable uncertainty assessment in hydrology, and the complexity of rainfall and runoff, respectively (Singh 2011, Liu et al. 2013, Chou 2014).

According to the literature, this research is unique since Cross-Sample Entropy (Cross-SampEn) has not been used for hydrology or climate analysis. Richman and Moorman (2000) developed Cross-SampEn to identify the degree of conformity or likeness between bivariate time series (Richman & Moorman 2000). Cross-SampEn is an improvement of the Cross-ApEn index developed by Pincus (1991) (Pincus 1991). As a result, Cross-SampEn is utilized in this study to establish synchronization between hydro-climatic time series and to identify the effects of climate change on low streamflow fluctuations in Iran.

The Middle East is expected to experience more intense warming than the whole of the world. Climate models predict global aridity, increasing the frequency and severity of droughts across the region. That means the majority of river systems and water resources will be influenced. Iran will face a major disaster due to the region becoming hotter and drier than the rest of the Middle East (an increase of 2.6°C in mean temperatures and a 35% decrease in precipitation) (Mansouri Daneshvar et al. 2019, Bozorg-Haddad et al. 2020).

The Namak-Lake basin is one of the largest, populated, and momentous basins located in Central Iran. Due to the development programs, rising demand for water, and being located in the arid and semi-arid zones, water scarcity has raised the most vital and challenging issue confronting this basin. In recent years, various projects have been implemented to control, store, transfer and manage water resources. This package of measures resulted in the Namak Lake basin having the most complex hydrological system in Iran. Also, the variations in topographic, climatic, geologic, and hydrologic conditions have added to the complexity of this basin. It must be considered that planning, management, and optimal exploitation of water resources in an arid and semi-arid region facing water scarcity and climate change are of crucial importance. However, lack/insufficiency of data in arid and semi-arid regions caused interactions between hydro-climatic parameters to remain unknown.

This study aims to investigate the observed spatio-temporal variations in climate parameters and low streamflow indices and evaluate the climate change effects on identified low streamflow fluctuations in a case study in the Namak Lake basin. Among the specific aims are the following: (1) to examine the annual/seasonal temperature and rainfall features, as well as seasonal low streamflow indicators, in Iran's Namak Lake basin from 1970 to 2015; (2) to use statistical approaches to identify probable changes in hydro-climatic characteristics as a result of climate change; (3) to establish relationships and associations between climatic factors and seasonal low streamflows and possible climate change utilizing both traditional and Cross-SampEn statistical methods.

2. Material and methods

2.1. Study Region

The Namak Lake basin is located in the center of Iran, with the geographic coordinates of 48° 20' to 52° 40' E and 32° 00' to 36° 30' N (Fig.1) and covers an area of 92,560 km^2. The Namak Lake Basin is one of Iran's largest and most densely populated river basins (5.6% of the total area and 20% of the total population of Iran) with the most complex hydrological system in the country.

A wide range of height differences from the uplands (Hmax= 4300 m located in the Alborz mountains) to the lowlands (Hmin= 800 m located in the Namak Lake) caused a great variety of climates the studied region. The climates include arid (lowlands) in large parts and semi-arid to humid (highlands) in small parts of the basin. Rainfall values decrease from the west to the east and from the north to the south of the basin due to extreme geomorphological anomalies and a decrease in the influence of air masses. Except for a small region in the highlands, rainfall varies from moderate to low in most of the basin. Following that, the precipitation regime shows a significant variation based on the isolines map, with the highest and lowest values recorded in the highland Alborz Mountains (1000mm) and the basin's eastern part (100mm), respectively. As with rainfall, temperature varies widely, with greater volatility in the eastern and central parts of the basin than in the western part. Under the influence of height variation, the mean temperature varies between 6 and 19 °C in the basin. The basin's average rainfall and mean temperature were estimated to be approximately 274 mm/year and 13 °C, respectively.

2.2. Data Sets

The river network in the Namak Lake basin consists of six main rivers, including Shoor, Jajrood, Karaj, Qara-Chai, Qom-Rood, and Bon-Rood. Daily mean discharge data were collected from 197 gauging stations established by the Ministry of Energy (MOE). In addition, for conducting the statistical analysis of the climatic parameters, rainfall and temperature datasets were collected from MOE and I.R.OF IRAN Meteorological Organization (IRIMO), including 284 weather stations (rain and evaporation gauges and synoptic stations). The daily data suffer from sufficient/varied length/poor quality observation. Therefore, the hydroclimatic data was checked in terms of quality, accuracy, data missing, outliers, etc. The datasets of temperature, rainfall, and streamflow with a maximum record length of 46 years (1970-2015) were used in this study. The characteristics of the selected gauging stations are shown in Tables 1 and 2. Fig.1 represents the spatial distribution of the selected gauging stations in the Namak Lake Basin.

The low stream flows were determined using the Indicators of Hydrologic Alteration (IHA) software. The low streamflow was defined as the lowest average streamflow measured over a continuous n-day period (Dudley et al. 2020).

2.3. Statistical Methods

This study evaluated the long-term changes in hydro-climatic time series to demonstrate the presence of climate change in the Namak Lake basin. Then, the impacts of long-term climatic parameter fluctuations on low streamflows were investigated.

In the first step, the spatio-temporal changes in long-term hydro-climatic time series have been identified to investigate and determine any impact of climate change on low streamflows. Significant changes in hydro-climatic time series are examined using both parametric and non-parametric approaches. Non-parametric methods are more appropriate for series with an abnormal distribution and are less sensitive to missing data and extreme values in time series. Because hydro-climatic series often follow a non-normal distribution, non-parametric tests have been appropriate for this purpose (Yue et al. 2002). The Modified-Mann-Kendall (MMK) test (Hamed and Ramachandra Rao, 1998) was applied as a non-parametric approach. Sen's Slope Estimator method (SSE) is used to estimate the actual slope of the trend in the low streamflow series. This method was first developed by Theil (1950) and was discussed by Sen (1968). As with the MMK test, this approach is based on a comparison of observed time series. In addition, the linear regression method was utilized to find trends in climatic time series and determine the magnitude of the significant trend based on the slope as a measure of the variable's average temporal variation (Tabari & Talaee 2011). The significance values $\alpha = 0.01$ and 0.05 were used in this study.

The effects of climatic parameters on low streamflow changes are determined in the second step. Various physical and climatic parameters influence the low streamflow due to its complex and multi-dimensional structure. Identification and knowledge of effective parameter changes and their relationships are vital to managing, planning, and forecasting low streamflow. To this end, traditional approaches (Spearman correlation coefficient) and novel methods (Cross-SampEn) are used to extract the connections and associations between them. Fig. 2 shows the flowchart of this study.

2.3.1. Association Analysis

The two most popular methods for determining the linear and nonlinear dependence between any pair of variables are the Pearson and Spearman correlation coefficients (Konapala et al., 2018). The Pearson correlation coefficient is not robust and stable. If the nonlinear connection, even robust connections cannot be identified and may be exceedingly sensitive to outlier pairs. The Pearson correlation coefficient is suitable for linear associations, while the Spearman correlation coefficient is probable for monotone relationships (Wilks 2019).

The basic assumption of the Pearson correlation coefficient is that pair variables have a Gaussian distribution (von Storch 1999), whereas, in the Spearman correlation coefficient, it is not necessary to assume that the variables follow a Gaussian distribution (Kahya & Kalaycı 2004). Hence, the Spearman correlation coefficient and a nonlinear cross-entropy method were employed in this study.

2.3.1.1. Cross-SampEn

Entropy is an information measure for recognizing the complexity of a system (Shannon 1948). Pincus (1991) represented the Approximate Entropy (ApEn) measure that quantifies the complexity and degree of the time series disorder.

Richman and Moorman (2000) identified the weaknesses of the ApEn method and developed the Sample Entropy (SampEn) algorithm that is the improved ApEn. SampEn, like ApEn, is a statistic of self-heterogeneity in a time series. On the other hand, SampEn was developed to reduce bias and not count self-matches compared to ApEn (Richman & Moorman 2000). Then, Richman and Moorman (2000) proposed the cross-sample entropy (Cross-SampEn) method to quantify the asynchrony between two dependent time series. The Cross-SampEn measure estimates a positive value for each time series, with a higher value indicating higher heterogeneity and a lower value indicating higher conformity. Further details on Cross-SampEn can be found in Richman and Moorman (2000), and Appendix (A).

3. Results

3.1. Long-term variations in seasonality low streamflow

Determination of low streamflow seasonality indices is carried out based on hydrographs and rainy/non-rainy seasons, as shown in Fig. 3. For this purpose, two seasons were specified: summer (June-November) and winter (December-May). Then, 1-day, 3-day, and 7-day minimum streamflows were calculated based on two seasons for the selected stations over 1970-2015.

Summer and winter have the highest and lowest rainfall amounts in the region, respectively, as seen in Fig. 3 (rainfall starting in November and ending in May). However, rainfall was not uniformly distributed over the basin. The Hamadan station in the west and the Kashan station in the east, for example, display the highest and minimum rainfall amounts, respectively. Based on Fig. 3, although the same temperature patterns are displayed, the difference in their values is recorded in the basin. For example, eastern stations (Kashan) have warmer patterns than western ones (Hamadan).

The MMK test and SSE were used to examine the long-term changes in low streamflow seasonality indices (Fig. 4). As illustrated in Fig.4, a significant declining trend in the low streamflow seasonality indices was detected for over 55% of stations.

The spatial distribution of the long-term variations in 1, 3, and 7-day seasonal low streamflows is presented in Fig. 5. Except in the northeastern part of the study region, Fig. 5 shows a clear decline in low streamflow seasonality indices during 1970-2015. In the northeastern part, the regime of rivers is snowy-rainy. So, the non-meaningful decreasing trend shows the influence of snow-melting on the base flow.

3.2. Long-term changes in climatic parameters

With less than one-third of annual global precipitation, Iran is located in the Middle East and has a large climatic variability. Over 85% of the area consists of an arid and semi-arid climate. The annual average precipitation is roughly 250 mm, with significant variations across the country and during the year (ranging from less than 50 mm to about 1000 mm) (Madani 2014). Iran is currently experiencing a water crisis, according to the situation. Additionally, hydro-climatic studies and climate change projections indicate that the Middle East's annual precipitation will decline by 5 to 25%. In Iran, this yearly precipitation decline is forecasted to be between 20% and 25% (Bozorg-Haddad et al. 2020).

3.2.1. Long-term changes in rainfall

According to Fig. 6, negative and positive trends in annual rainfall were observed at the 57 gauge stations and a clear directional trend was not apparent. The magnitude ranges of the decreasing and positive trends in annual rainfalls obtained between (-) 0.7 to (-) 4.3 mm/year and (+) 1.1 to (+) 4.5 mm/year, respectively.

In terms of seasonal rainfall, a non-significant declining trend was observed in a large number of stations during the winter rainfall (in 57% of stations). In addition, a significant increase was identified in the summer and fall rainfall (in 29% and 21% of stations, respectively).

As seen in Fig.7, the annual and spring rainfall variations are not uniform or homogeneous throughout the Namak Lake Basin. The increasing tendency was observed during the fall and summer rainfall, in contrast to the dominant decreasing trend that was determined during the winter rainfall.

3.2.2. Long-term variations in temperature

According to Fig. 8, the warming trend was observed in 92% of the studied stations in all series, although the percentage of stations with a significant increasing trend was different in each series. Additionally, the maximum magnitude of the significant increasing trend of T_{mean} was determined to be (+) 0.1 °C and (+) 0.04 °C per decade in the fall and warm seasons, respectively.

As illustrated in Fig.9, an increasing trend was identified as a dominant pattern across the study area.

3.3. The estimation of association among hydro-climatic indices

3.3.1. Application of Spearman correlation method

3.3.1.1. The association between seasonal rainfall and low streamflow

Spearman's correlation coefficient was used to recognize the relationships between variability of low streamflow seasonality indices and climate parameters at 90 and 95% confidence levels. The Spearman test obtained is shown in Fig.10 and Fig. 11.

According to Fig. 10, winter low streamflow indices have the most significant correlation with fall rainfall and no significant correlation with winter/spring rainfall. The significant associations with fall and annual rainfall range from 0.3 to 0.5 and (-) 0.3 to 0.4. According to Fig. 10, summer low streamflow indices have a higher correlation with winter and annual rainfall, while there is no significant correlation with fall rainfall. The significant associations with winter and annual rainfall range from 0.3 to 0.4.

The correlations between seasonal rainfall and the 7-day winter low streamflow time series were more remarkable than other low streamflow indices. The 7-day winter low streamflow time series showed significant correlations with fall rainfall time series, ranging from 0.3 to 0.5, in more than 38% of all selected stations. The significant annual rainfall correlations, ranging from (-) 0.3 to 0.4, were observed in 33% of all considered stations.

The highest correlation was found in winter and annual scales based on the summer low streamflow indices. The 7-day summer low streamflow time series showed significant positive correlation values with the winter rainfall time series, ranging from 0.3 to 0.4, with a variance of about 12 - 22%. The annual rainfall time series showed a significant positive correlation, ranging from 0.3 to 0.4, in 27% of all stations.

3.3.1.2. The association between seasonal temperature and low streamflow

The graphical results for the correlation coefficients of temperature and winter low streamflow series are given in Fig. 11. For all series, a dominant-negative association between temperature series and low streamflow seasonality indices was observed. Based on Fig. 11, winter low streamflow indices showed a strong negative significant correlation with summer temperature (in 33 - 44% of stations) and a weak negative significant correlation with winter/spring temperature series (in 5 - 16% of stations).

Summer low streamflow indices demonstrated a strong negative significant correlation with the annual temperature series (in 50 - 55% of stations) and the lowest significant correlation with the spring temperature series (in 5% of stations).

3.3.2. Application of Cross-SampEn method

The atmosphere is a dynamic, non-linear and chaotic system. Complexity, non-linearity, and non-stationarity are the important attributes of these parameters. Cross-SampEn calculates a positive measure of similarity, with smaller values indicating greater similarity and larger values indicating significant heterogeneity. Tables 3 and 4 give the summarized results of Cross-SampEn in the Namak Lake Basin.

According to Table 3, the varied values of Cross-SampEn at the various time scales of interest suggest the presence of significant inter-seasonal/inter-annual fluctuations in climatic and hydrologic parameters depending on time and location. Cross-SampEn values were lowest and highest during the dry season (summer) and annual rainfall series, respectively. We excluded summer rainfall due to its low amount (2% of total) and its little effect on the low streamflow. The values of Cross-SampEn suggest a very distinct degree of rainfall distribution and variation during the annual rainfall.

According to Table 3, summer low streamflow is more associated with temperature than winter low streamflow (lowest Cross-SampEn value). The minimum value of the Cross-SampEn for temperature was not observed during the same period for winter/summer low streamflow. On the contrary, the fall temperature has the maximum values of the variation coefficient in the winter/summer low streamflow time series.

During the seasonal and annual periods, the variation of temperature entropy values was lower than rainfall entropy values because of the existing small inter-annual and inter-seasonal variation in temperature time series.

Overall, the entropy values of rainfall time series were larger than those of temperature time series since rainfall variation is more severe than temperature variation, especially in arid and semi-arid regions. The synchrony and correlation between bivariate low streamflow and rainfall time series were quantified by using Cross-SampEn. A summary of the results for the 18 hydrometric stations is shown in Fig. 12.

According to the findings of Cross-SampEn, the winter rainfall time series showed the most similarity to the summer/winter low streamflow in the majority of stations. The minimum entropy value of the winter low streamflow was obtained with the winter and spring rainfall time series, respectively (44-55% and 28% of stations). The summer low streamflow also showed a correlation with the winter rainfall time series. The minimum entropy value of the summer low streamflow time series was obtained with the winter rainfall time series in 44% of stations and the autumn rainfall time series in 28% of stations.

Fig. 13 represents the Cross-SampEn values of annual and seasonal temperature and winter/summer low streamflow at 18 hydrometric stations located in the Namak Lake basin. According to the results of cross-SampEn, the annual temperature showed the highest correlation with seasonal low streamflows in the majority of the selected stations. The minimum entropy value of winter low streamflow was obtained at an annual temperature of 44-55% of stations and a fall temperature in 27% of stations. The summer low streamflow showed a strong correlation with the summer and annual temperature. The minimum entropy value of 1-day summer low streamflow was obtained at summer temperature in 66% of stations. This value for 3-day and 7-day summer low streamflow was obtained in summer, and the annual temperature in 55% and 38% of stations, respectively.

4. Discussion

In arid and semi-arid regions, streamflow responses to climate change are more pronounced, as a little climate oscillation can produce a vast range of changes (Ling et al. 2013; Sheikh et al. 2020).

4.1. Low streamflow and climatic parameters changes

Exploration of the long-term changes in seasonal low streamflow indices showed decreasing trends in the study region. The greatest magnitude of diminishing trends was reported to be (-) 0.02 m^3/s per decade for the 1, 3, and 7-day summer low streamflow. For 1, 3, and 7-days of winter low streamflow, these values were (-) 0.02, (-) 0.03, and (-) 0.04 m^3/s per decade, respectively.

The summer low streamflow accounted for a greater proportion of the severity of the observed decreasing trend than the winter low streamflow (82% of the significant declining trend at the 1% probability level). During the summer season, as a result of the combined effects of low rainfall, increasing radiation, high evapotranspiration, and non-drainage of groundwater, the lowest value of streamflow in rivers, particularly seasonal rivers, is observed. Additionally, increased agricultural water demand in this season has resulted in an overuse of surface and groundwater resources.

The drastic significant variations in seasonal low streamflow time series are generally associated with climate change and/or human interventions. The long-term temporal variation of seasonal rainfall revealed a strong significant declining trend in the winter rainfall time series (45% of stations). The range magnitude of a meaningful diminishing trend in winter rainfall was obtained

(-) 0.3 to (-) 3.8 mm/season per year. Tabari and Talaee (2011) discovered a decreasing tendency in winter rainfall at 60% of stations in Iran, a trend that was significantly stronger than other season scales.

In the Namak Lake basin, winter and spring contribute the most to annual rainfall totals. Therefore, the drop in the winter and spring rainfall has had a meaningful influence on streamflow reduction during water deficit periods. It is worth noting that groundwater significantly contributes to river discharge during drought and water deficit periods (Smakhtin 2001). Winter rainfall is one of the main sources of recharge for the Namak Lake Basin's aquifers. Thus, a diminishing in winter rainfall due to influence on aquifer recharge can alter the frequency of low streamflows during drought periods.

Long-term variation in the T_{mean} time series has revealed a dominant increasing trend, particularly in the annual and winter series (over 70% of stations). By increasing the winter temperature, it could be affected by rainfall quantity and type. Furthermore, declining effective rainfall has reduced water loss and aquifer recharge. The time of snow-melting in snowy basins has changed and shifted, resulting in a dramatic increase in the river network's streamflow. By contrast, during dry periods, it faces a more severe streamflow shortage. On the other hand, rising summer temperatures will increase water demand, resulting in increased evapotranspiration and decreased streamflow.

4.2. Estimation of the association between climatic parameters and low streamflows

According to this study's findings, winter and spring rainfall are likely to affect changes in low streamflows in rivers. This is because, during the rainy season, the streamflow response is more sensitive to rainfall variations (Li et al. 2014). Winter and spring rainfall effects were evaluated, and both approaches indicated the highest association between winter rainfall and seasonal low streamflows, particularly the entropy method. The same patterns of relationships between seasonal rainfall and low streamflows were recognized in Cross-SampEn, with the winter, fall, and spring having the highest correlation in both series of low streamflow indices, respectively.

According to Spearman’s rank correlation statistics, no notable association between winter/spring rainfall and winter low streamflow was identified. However, the Cross-SampEn analysis revealed the most coherency and similarity between winter and fall rainfall and summer low streamflow. It should be emphasized that the rainfall seen in the Namak Lake Basin is primarily in the form of rain, while snowfall is quite rare in mountain basins. As a result, the basin's response to rainfall is projected to be more rapid and visible in streamflow.

The influential role of winter rainfall on low streamflows and its decreasing trend during the last four decades can be one of the effective reasons for the diminishing trend of low streamflows in the Namak Lake basin. Sheikh et al. (2020) also reported the variations in the seasonal rainfall and rainfall regime ratio in the Namak Lake basin. Also, a meaningful declining trend was found in March as one of the most productive months of the year that has a probable influence on the low streamflows.

We believe the streamflow in a particular month is not entirely dependent on the rainfall in that month. It is often the response of a combined influence (with a lag time) of rainfall in that month and other months (Masih et al. 2011). However, the significant relation between winter rainfall and summer low streamflow can be due to slowly occurring groundwater flow systems. Groundwater abstraction is essential to source supplies to the discharge of a river network during drought and continuous dry periods (Smakhtin 2001). 29% of the total basin area consists of aquifers and, 122424 groundwater resources (including springs, wells, and qanats) exist around the Namak Lake Basin, according to official statistics (Abkhan Consulting Engineers 2013).

The findings derived from the linkage between temperature and seasonal low streamflow indices were similar. Both association analysis methods showed that the annual and summer temperatures have the main effect on the low streamflow indices. Increasing evapotranspiration as a result of rising temperatures with increased demand for water in agriculture can have a direct effect on the streamflow. However, it should be considered that more parameters in addition to temperature had effects on increasing evapotranspiration. In this study, the Spearman method identifies an inverse relationship between seasonal temperature and low streamflow, but the Cross-SampEn method cannot determine the direction of the relationship. That is one of the limitations of this method.

Masih et al. (2011) studied streamflow trends of the Karkheh River in Iran and their correlation with temperature and rainfall. They recognized a declining trend in low streamflow and stated that the changes in climatic parameters, especially the changes in rainfall, caused a declining trend in streamflow. In contrast, Ling et al. (2012) identified a significant increasing trend in the low streamflows, temperatures, and rainfall during 1957-2007 in the headstream of the Tarim River. The results showed that temperature had more influence on low streamflow than rainfall.

5. Conclusion

In arid locations with fragile ecosystems, even little changes in the climate can significantly impact on the ecosystem’s water balance. The Namak Lake basin has been experiencing water stress in recent years as a result of climate variability, factors governing it, inappropriate development programs, and over-capacity pressure on water resources.

According to the findings of this study, rainfall showed a greater influence on low streamflows in the study region than temperature. The study of the findings obtained using the Spearman and Cross-SampEn methods revealed a significant difference in the performance of the two methods. It is worth noting that low streamflows are more nonlinearly related to climate indices (Konapala et al. 2018). As a result, it is believed that entropy results will be more accurate. However, the existing uncertainty in the results is irrefutable. The length of the statistical period, the limited number and distribution of selected stations, data quality, and missing data are all significant sources of uncertainty when using these approaches, all of which contribute to the uncertainty in the results.

As a result, it is critical to note that the relationships between hydro-climatic factors vary between time scales and geographical locations. In heterogeneous regions, the variability of physical (including physiography, geomorphology, geology, and topography) and climatic variables influences the development of low streamflows in diverse basin sections.

However, the detection of a significant correlation between rainfall/temperature and low streamflow was weak, emphasizing the role of the other effective parameters. Because the complicated processes that generate low streamflows are controlled by various geological, topographic, and climatic factors, rainfall/temperature has only a portion of the contribution to the generation of low streamflows.

On the other hand, according to Yang et al. (2010), in addition to climatic parameters, it is necessary to consider the abstraction of groundwater, the role of human activities, especially the existence of numerous structures for controlling and storing surface water for agricultural and industrial purposes, and inter-basin water transfer (IBT) as well as geomorphology, land cover and land use, because climate change and human activities (deforestation, reforestation, urbanization, agriculture, dams, etc.) are more effective at low streamflow events than high streamflow events (Zhang et al. 2009).

Basins are complex hydrological systems composed of many input and output variables. Complexity, non-linearity, and non-stationary relationships between variables in the hydrological systems are the primary attributes that complicate their research. The results, however, showed that the Cross-SampEn method has more favorable potential for hydro-climatic studies than conventional linear/nonlinear methods.

Acknowledgement

We would like to express our special appreciation and thanks to Dr. Mostafa Rostaghi for his great assistance with the Cross-Entropy methods used in this article. And we wish to thank Professor Paul J. DuBowy for his brilliant review of the manuscript and constructive comments and suggestions.

References

Abkhan Consulting Engineers (2013) Updated studies for balancing of water resources in the studied regions of Namak Lake Basin.

Ali R, Kuriqi A, Abubaker S, Kisi O (2019) Long-term trends and seasonality detection of the observed flow in Yangtze River using Mann-Kendall and Sen’s innovative trend method. Water (Switzerland) 11:1855.

Assani AA, Chalifour A, Légaré G, Manouane C-S, Leroux D (2011) Temporal Regionalization of 7-Day Low Flows in the St. Lawrence Watershed in Quebec (Canada). Water Resour Manag 25:3559–3574.

Bozorg-Haddad O, Zolghadr-Asli B, Sarzaeim P, Aboutalebi M, Chu X, Loáiciga HA (2020) Evaluation of water shortage crisis in the Middle East and possible remedies. J Water Supply Res Technol -

AQUA 69:85–98.

Cammalleri C, Vogt J, Salamon P (2017) Development of an operational low-flow index for hydrological drought monitoring over Europe. Hydrol Sci J 62:346–358.

Chou CM (2014) Complexity analysis of rainfall and runoff time series based on sample entropy in different temporal scales. Stoch Environ Res Risk Assess 28:1401–1408.

Degefu MA, Bewket W (2017) Variability, trends, and teleconnections of stream flows with large-scale climate signals in the Omo-Ghibe River Basin, Ethiopia. Environ Monit Assess 189:142.

Dudley RW, Hirsch RM, Archfield SA, Blum AG, Renard B (2020) Low streamflow trends at human-impacted and reference basins in the United States. J Hydrol 580:124254.

Fangmann A, Haberlandt U (2019) Statistical approaches for identification of low-flow drivers: Temporal aspects. Hydrol Earth Syst Sci 23:447–463.

Foulon É, Rousseau AN, Gagnon P (2018) Development of a methodology to assess future trends in low flows at the watershed scale using solely climate data. J Hydrol 557:774–790.

Ghafouri-Azar M, Kim JB, Bae DH (2021) Assessment of the potential changes in low flow projections estimated by Coupled Model Intercomparison Project Phase 5 climate models at monthly and seasonal scales. Int J Climatol 41:3222–3236.

Giuntoli I, Renard B, Vidal JP, Bard A (2013) Low flows in France and their relationship to large-scale climate indices. J Hydrol 482:105–118.

Hamed KH, Ramachandra Rao A (1998) A modified Mann-Kendall trend test for autocorrelated data. J Hydrol 204:182–196.

Jehanzaib M, Sattar MN, Lee JH, Kim TW (2020) Investigating effect of climate change on drought propagation from meteorological to hydrological drought using multi-model ensemble projections. Stoch Environ Res Risk Assess 34:7–21.

Kahya E, Kalaycı S (2004) Trend analysis of streamflow in Turkey. J Hydrol 289:128–144.

Konapala G, Valiya Veettil A, Mishra AK (2018) Teleconnection between low flows and large-scale climate indices in Texas River basins. Stoch Environ Res Risk Assess 32:2337–2350.

Kuriqi A, Ali R, Pham QB, Montenegro Gambini J, Gupta V, Malik A, Linh NTT, Joshi Y, Anh DT, Nam VT, Dong X (2020) Seasonality shift and streamflow flow variability trends in central India. Acta Geophys 68:1461–1475.

Lake DE, Richman JS, Griffin MP, Moorman JR (2002) Sample entropy analysis of neonatal heart rate variability. Am J Physiol Integr Comp Physiol 283:R789–R797.

Lee T, Ouarda TBMJ, Yoon S (2017) KNN-based local linear regression for the analysis and simulation of low flow extremes under climatic influence. Clim Dyn 49:3493–3511.

Li F, Zhang G, Xu YJ (2014) Spatiotemporal variability of climate and streamflow in the Songhua River Basin, northeast China. J Hydrol 514:53–64.

Ling H, Xu H, Fu J (2013) High- and low-flow variations in annual runoff and their response to climate change in the headstreams of the Tarim River, Xinjiang, China. Hydrol Process 27:975–988.

Liu B, Chen X, Lian Y, Wu L (2013) Entropy-based assessment and zoning of rainfall distribution. J Hydrol 490:32–40.

Liu L-Z, Qian X-Y, Lu H-Y (2010) Cross-sample entropy of foreign exchange time series. Phys A Stat Mech its Appl 389:4785–4792.

Madani K (2014) Water management in Iran: what is causing the looming crisis? J Environ Stud Sci 4:315–328.

Mahmoodi N, Wagner PD, Kiesel J, Fohrer N (2020) Modeling the impact of climate change on streamflow and major hydrological components of an Iranian Wadi system. J Water Clim Chang.

Mansouri Daneshvar MR, Ebrahimi M, Nejadsoleymani H (2019) An overview of climate change in Iran: facts and statistics. Environ Syst Res 8:1–10.

Marx A, Kumar R, Thober S, Rakovec O, Wanders N, Zink M, Wood EF, Pan M, Sheffield J, Samaniego L (2018) Climate change alters low flows in Europe under global warming of 1.5, 2, and 3°C. Hydrol Earth Syst Sci 22:1017–1032.

Masih I, Uhlenbrook S, Maskey S, Smakhtin V (2011) Streamflow trends and climate linkages in the Zagros Mountains, Iran. Clim Change 104:317–338.

Pincus SM (1991) Approximate entropy as a measure of system complexity. Proc Natl Acad Sci U S A 88:2297–2301.

Richman JS, Moorman JR (2000) Physiological time-series analysis using approximate entropy and sample entropy. Am J Physiol Circ Physiol 278:H2039–H2049.

Sen PK (1968) Estimates of the Regression Coefficient Based on Kendall's Tau. J Am Stat Assoc 63:1379.

Shannon CE (1948) A Mathematical Theory of Communication. Bell Syst Tech J 27:379–423 & 623–656.

Sheikh Z, Yazdani MR, Moghaddam Nia A (2020) Spatiotemporal changes of 7-day low flow in Iran's Namak Lake Basin: impacts of climatic and human factors. Theor Appl Climatol 139:57–73.

Shen Y-J, Shen Y, Fink M, Kralisch S, Chen Y, Brenning A (2018) Trends and variability in streamflow and snowmelt runoff timing in the southern Tianshan Mountains. J Hydrol 557:173–181.

Singh VP (2011) Hydrologic Synthesis Using Entropy Theory : Review. J Hydrol Eng.

Smakhtin VU (2001) Low flow hydrology: A review. J Hydrol 240:147–186.

von Storch H (1999) Misuses of Statistical Analysis in Climate Research. Anal Clim Var:11–26.

Tabari H, Talaee PH (2011) Temporal variability of precipitation over Iran: 1966-2005. J Hydrol 396:313–320.

Theil H (1950) A rank-invariant method of linear and polynomial regression analysis, 3; confidence regions for the parameters of polynomial regression equations. Sticht Math Centrum Stat Afd.

Tomaszewski E, Kubiak-Wójcicka K (2021) Low-Flows in Polish Rivers. Springer, Cham, p 205–228

Vlach V, Ledvinka O, Matouskova M (2020) Changing low flow and streamflow drought seasonality in central european headwaters. Water (Switzerland) 12:3575.

Wang H, Stephenson SR, Qu S (2020) Quantifying the relationship between streamflow and climate change in a small basin under future scenarios. Ecol Indic 113:106251.

Wilks DS (2019) Statistical Methods in the Atmospheric Sciences, Fourth Edi. Elsevier.

Yang T, Xu C-Y, Shao Q, Chen X, Lu G-H, Hao Z-C (2010) Temporal and spatial patterns of low-flow changes in the Yellow River in the last half century. Stoch Environ Res Risk Assess 24:297–309.

Yue S, Pilon P, Cavadias G (2002) Power of the Mann-Kendall and Spearman's rho tests for detecting

monotonic trends in hydrological series. J Hydrol 259:254–271.
Zhang Q, Xu C-Y, Yang T (2009) Variability of water resource in the Yellow River Basin of past 50 years, China. Water Resour Manag 23:1157–1170.

Table 1 The properties of the selected streamflow gauging stations in the Namak Lake Basin (during 1970-2015)

Number	Station ID	Station	River	Drainage Area (Km^2)	Elevation (m)	Longitude (E)	Latitude (N)	Q_{Annual} (m^3/s)	Q_{Min} (m^3/s)	Q_{Max} (m^3/s)	Volume (MCM)
1	41005	Ghamsar	Bon-Rood	68	1976	51° 25´	33° 43´	0.10	0.02	0.30	3.19
2	41009	Sarab-Hende	Golpayegan	816	2010	50° 02´	33° 23´	3.49	0.52	11.85	110.12
3	41035	Yalfan	Abshineh	165	1980	48° 36´	34° 43´	1.55	0.57	3.17	48.76
4	41041	Soolan	Mariyanj	37	1979	48° 25´	34° 49´	0.38	0.14	0.75	11.91
5	41043	Saleh-Abad	Saleh-Abad	180	1770	48° 20´	34° 55´	1.09	0.13	2.33	34.29
6	41045	Bahadorbeic	Bahadorbeic	200	1780	48° 19´	34° 57´	0.87	0.12	2.10	27.37
7	41049	Khomeygan	Khomeygan	225	1840	49° 01´	35° 22´	0.37	0.02	2.38	11.70
8	41051	Zehtaran	Zehtaran	372	1770	49° 08´	35° 15´	0.27	0.10	0.68	8.52
9	41053	Omar-Abad	Qara-Chai	14277	1590	49° 14´	35° 06´	6.28	0.01	30.63	197.96
10	41055	Jalayer	Qara-Chai	17236	1200	50° 01´	34° 52´	7.28	1.21	19.12	229.46
11	41059	Razin	Mazlaghan	2174	1300	50° 00´	35° 01´	2.22	0.58	4.64	69.96
12	41067	Abgarm	Khar-Rood	2472	1560	49° 17´	35° 45	2.81	0.37	6.85	88.66
13	41071	Rahim-Abad	Khar-Rood	4051	1390	49° 32´	35° 52´	3.87	0.01	11.66	122.07
14	41095	Deh-Someh	Kordan	360	1410	50° 50´	35° 57´	3.55	1.10	6.61	111.89
15	41099	Pol-Asef-al Doleh	Shoor	17100	1122	50° 45´	35° 41´	1.95	0.01	18.44	61.44
16	41101	Siera	Karaj	730	1790	51° 08´	36° 01´	12.53	6.85	19.90	395.14
17	41109	Soleghan	Kan	200	1430	51° 15´	35° 46´	2.46	0.53	4.80	77.55
18	41117	Roodak	Jajrood	762	1690	51° 32´	35° 51´	7.70	3.07	14.74	242.81

Table 2 The properties of the selected meteorological gauging stations in the Namak Lake Basin (during 1970-2015)

Station ID	Station	Type of Station	Elevation (m)	Longitude (E)	Latitude (N)	Annual Rainfall (mm)
41003	Fin	Evaporation Gauge	1045	51° 23´	33° 58´	145.74
41009	Sarab-Hende	Evaporation Gauge	2010	50° 02´	33° 23´	456.30
41512	MohammadAbad-Kashan	Evaporation Gauge	970	51° 45´	33° 52´	126.31
41103	Bileqan	Evaporation Gauge	1360	51° 02´	35° 49´	328.31
41117	Rudak	Evaporation Gauge	1760	51° 33´	35° 51´	277.86
41119	Latyan	Evaporation Gauge	1660	51° 41´	35° 46´	411.62
41220	Sorhe	Rainfall Gauge	1800	50° 56´	35° 57´	399.78
41232	AmirKabir Dam	Evaporation Gauge	1613	51° 05´	35° 57´	419.66
41236	Parandak	Evaporation Gauge	1040	51° 03´	35° 30´	169.22
41262	Garmabdar	Rainfall Gauge	2500	51° 37´	35° 59´	733.31
41292	Baqerabad	Rainfall Gauge	950	51° 34´	35° 24´	182.79
41332	Nesa	Evaporation Gauge	2270	51° 19´	36° 04´	676.15
41336	Shahrestanak	Evaporation Gauge	2150	51° 21´	35° 58´	639.47
41095	Dehsomeh	Evaporation Gauge	1410	50° 50´	35° 57´	319.25
41101	Siera	Evaporation Gauge	1790	51° 09´	36° 01´	612.36
41168	Kakajin	Rainfall Gauge	1770	49° 52´	36° 27´	577.92
41073	Qorveh	Rainfall Gauge	1420	49° 22´	36° 03´	293.86
41086	Top-Qareh	Rainfall Gauge	1850	48° 45´	36° 08´	362.53
41088	Dotappeh	Rainfall Gauge	1930	48° 49´	36° 07´	396.23
41116	Chargar	Rainfall Gauge	2000	49° 02´	36° 25´	348.55

Station ID	Station	Type of Station	Elevation (m)	Longitude (E)	Latitude (N)	Annual Rainfall (mm)
41618	Sain-Qaleh	Rainfall Gauge	1680	49° 04´	36° 18´	326.08
41067	Abgarm	Rainfall Gauge	1550	49° 17´	35° 45´	240.55
41069	Arteshabad	Rainfall Gauge	1750	49° 25´	35° 40´	267.56
41063	Pole-Arvan	Rainfall Gauge	1750	49° 11´	35° 37´	300.04
41071	Rahim-Abad	Rainfall Gauge	1400	49° 32´	35° 52´	317.36
41077	Nosrat-Abad-Hajiarab	Rainfall Gauge	1900	49° 37´	35° 33´	258.95
41079	Hajiarab	Evaporation Gauge	1670	49° 44´	35° 35´	273.27
41089	Behjat-Abad	Rainfall Gauge	1400	50° 22´	36° 08´	268.47
41091	Ziyaran	Rainfall Gauge	1620	50° 31´	36° 07´	354.21
41094	Dashtak	Rainfall Gauge	1700	48° 54´	35° 53´	309.41
41100	Gol-Cheshmeh	Rainfall Gauge	2200	49° 11´	35° 31´	496.07
41110	Parsbanaj	Rainfall Gauge	2250	49° 23´	35° 28´	437.38
41132	Ziaabad	Rainfall Gauge	1370	49° 27´	35° 59´	276.09
41140	Dial-Abad	Rainfall Gauge	1240	49° 47´	36° 04´	236.35
41144	Rudak-Qazvin	Rainfall Gauge	1520	49° 53´	35° 41´	577.70
41158	Ashtajin	Rainfall Gauge	1290	49° 45´	36° 14´	330.54
41164	Esmaeel-Abad	Rainfall Gauge	1270	49° 54´	36° 13´	334.54
41178	Nosrat-Abad	Rainfall Gauge	1190	50° 00´	36° 06´	261.01
41182	Mohammad-Abad-Khare	Rainfall Gauge	1180	50° 04´	36° 01´	251.60
41186	Mizouj	Rainfall Gauge	1800	50° 07´	36° 24´	458.74
41108	Quzlu	Evaporation Gauge	2000	49° 07´	35° 38´	415.77
41193	Mahmood-Abad	Rainfall Gauge	1650	49° 04´	35° 50´	272.07
41194	Kebrit-Mian	Rainfall Gauge	1450	50° 15´	36° 14´	318.25
41215	Morteza-Abad	Rainfall Gauge	1650	49° 48´	36° 24´	331.29
41630	Mahin	Rainfall Gauge	1600	49° 28´	36° 08´	304.82
41986	Deh-Arvan	Rainfall Gauge	1850	49° 10´	35° 37´	367.97
41040	Saruqbala	Evaporation Gauge	1800	49° 30´	34° 24´	247.68
41042	Ashtian	Evaporation Gauge	2080	50° 00´	34° 32´	241.57
41057	Band-Abbasi	Evaporation Gauge	1080	50° 08´	34° 54´	217.86
41082	Emam-Abad	Evaporation Gauge	920	50° 27´	34° 52´	182.37
41265	Ekbatan-Dam	Evaporation Gauge	1880	48° 36´	34° 45´	359.81
40769	Arak	Synoptic	1702	49° 46´	34° 04´	317.70
40767	Hamadan (Noje)	Synoptic	1679	48° 41´	35° 11´	319.87
40754	Tehran (Mehrabad)	Synoptic	1191	51° 18´	35° 41´	238.86
40770	Qom	Synoptic	879	50° 51´	34° 46´	140.38
40785	Kashan	Synoptic	955	51° 28´	33° 58´	136.38
40731	Qazvin	Synoptic	1279	50° 03´	36° 14´	320.34

Table 3 Summarized results of Cross-SampEn for seasonal rainfall and low streamflow series

Climatic Parameters	Winter Low Streamflow indices	Cross-SampEn statistics (bit)				Climatic Parameters	Summer Low Streamflow indices	Cross-SampEn statistics (bit)			
		Min	Max	Mean	SD			Min	Max	Mean	SD
Spring Rainfall	1-day	1.19	3.31	1.87	0.62	Spring Rainfall	1-day	0.44	1.82	1.03	0.35
	3-day	1.26	3.44	1.93	0.63		3-day	0.44	1.74	1.02	0.33
	7-day	1.30	3.46	1.90	0.52		7-day	0.44	1.58	0.99	0.31

Climatic Parameters	Winter Low Streamflow indices	Cross-SampEn statistics (bit)				Climatic Parameters	Summer Low Streamflow indices	Cross-SampEn statistics (bit)			
		Min	Max	Mean	SD			Min	Max	Mean	SD
Summer Rainfall	1-day	0.61	3.22	1.22	0.67	Summer Rainfall	1-day	0.25	1.51	0.56	0.29
	3-day	0.61	2.83	1.21	0.62		3-day	0.24	1.82	0.58	0.35
	7-day	0.62	2.59	1.20	0.52		7-day	0.24	1.76	0.56	0.31
Fall Rainfall	1-day	1.12	3.01	1.61	0.39	Fall Rainfall	1-day	0.35	1.19	0.78	0.23
	3-day	1.11	3.00	1.58	0.38		3-day	0.36	1.38	0.79	0.25
	7-day	1.01	2.43	1.52	0.30		7-day	0.36	1.39	0.81	0.24
Winter Rainfall	1-day	1.13	2.93	1.54	0.42	Winter Rainfall	1-day	0.48	1.29	0.78	0.20
	3-day	1.20	2.56	1.53	0.35		3-day	0.48	1.26	0.77	0.19
	7-day	1.23	2.19	1.52	0.28		7-day	0.48	1.16	0.77	0.17
Annual Rainfall	1-day	1.51	3.27	2.04	0.92	Annual Rainfall	1-day	0.75	2.63	1.50	0.52
	3-day	1.50	4.80	2.60	0.93		3-day	0.78	2.52	1.44	0.50
	7-day	1.36	4.55	2.39	0.80		7-day	0.79	2.49	1.41	0.48

SD: Standard Deviation

Table 4 Summarized results of Cross-SampEn for seasonal temperature and low streamflow series

Climatic Parameters	Winter Low Streamflow indices	Cross-SampEn statistics (bit)				Climatic Parameters	Summer Low Streamflow indices	Cross-SampEn statistics (bit)			
		Min	Max	Mean	SD			Min	Max	Mean	SD
Spring Temperature	1-day	1.36	3.24	2.02	0.88	Spring Temperature	1-day	0.58	2.24	1.37	0.52
	3-day	1.38	3.56	2.27	0.79		3-day	0.59	2.25	1.36	0.51
	7-day	1.35	4.29	2.54	0.72		7-day	0.55	2.13	1.31	0.47
Summer Temperature	1-day	1.22	3.77	2.28	0.70	Summer Temperature	1-day	0.49	2.42	1.10	0.43
	3-day	1.18	4.78	2.43	0.89		3-day	0.52	2.72	1.12	0.50
	7-day	1.18	3.71	2.22	0.71		7-day	0.54	2.71	1.10	0.47
Fall Temperature	1-day	1.40	3.85	2.18	1.26	Fall Temperature	1-day	0.46	2.93	1.53	0.68
	3-day	1.41	3.83	2.24	1.27		3-day	0.49	2.67	1.50	0.65
	7-day	1.40	4.38	2.40	1.39		7-day	0.49	2.57	1.41	0.61
Winter Temperature	1-day	1.45	5.09	2.38	1.03	Winter Temperature	1-day	0.69	2.26	1.44	0.49
	3-day	1.73	3.47	2.31	0.78		3-day	0.68	2.18	1.43	0.45
	7-day	1.69	3.00	2.27	0.70		7-day	0.70	2.16	1.40	0.44
Annual Temperature	1-day	1.34	3.89	2.27	0.71	Annual Temperature	1-day	0.40	1.65	1.11	0.36
	3-day	1.28	3.82	2.21	0.61		3-day	0.43	1.69	1.09	0.36
	7-day	1.33	3.66	2.21	0.61		7-day	0.48	1.80	1.10	0.36

SD: Standard Deviation

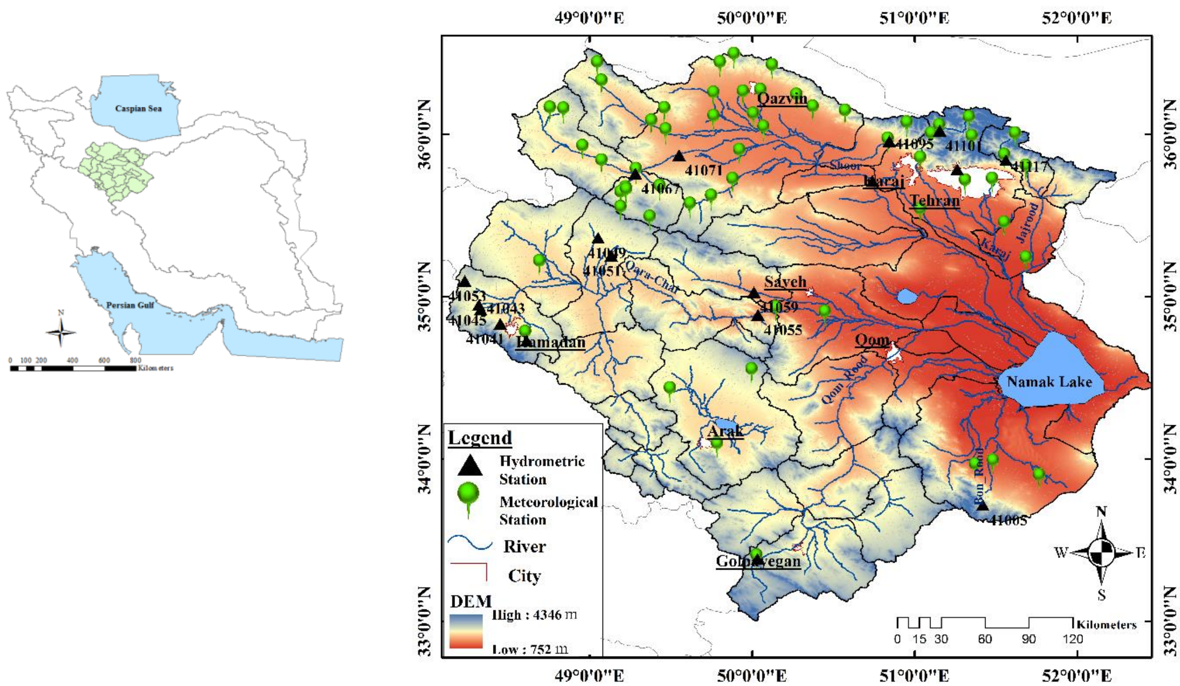

Fig. 1. Location of the Namak Lake Basin and the spatial distribution of the selected hydro-climatic gauging stations

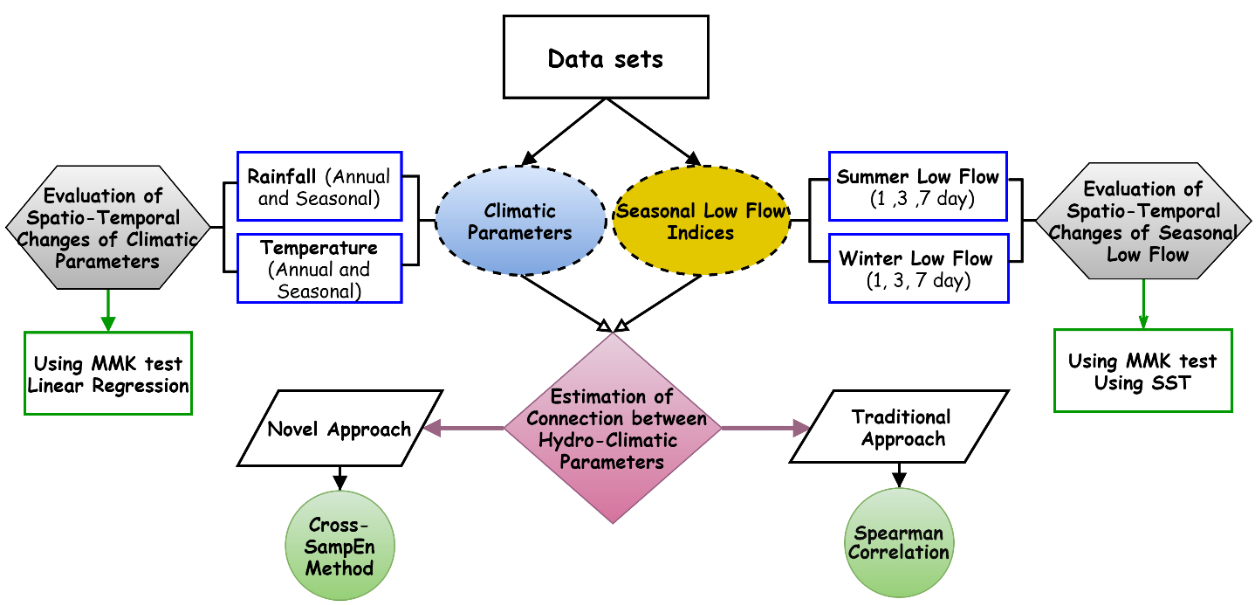

Fig. 2. Flowchart of the research methodology

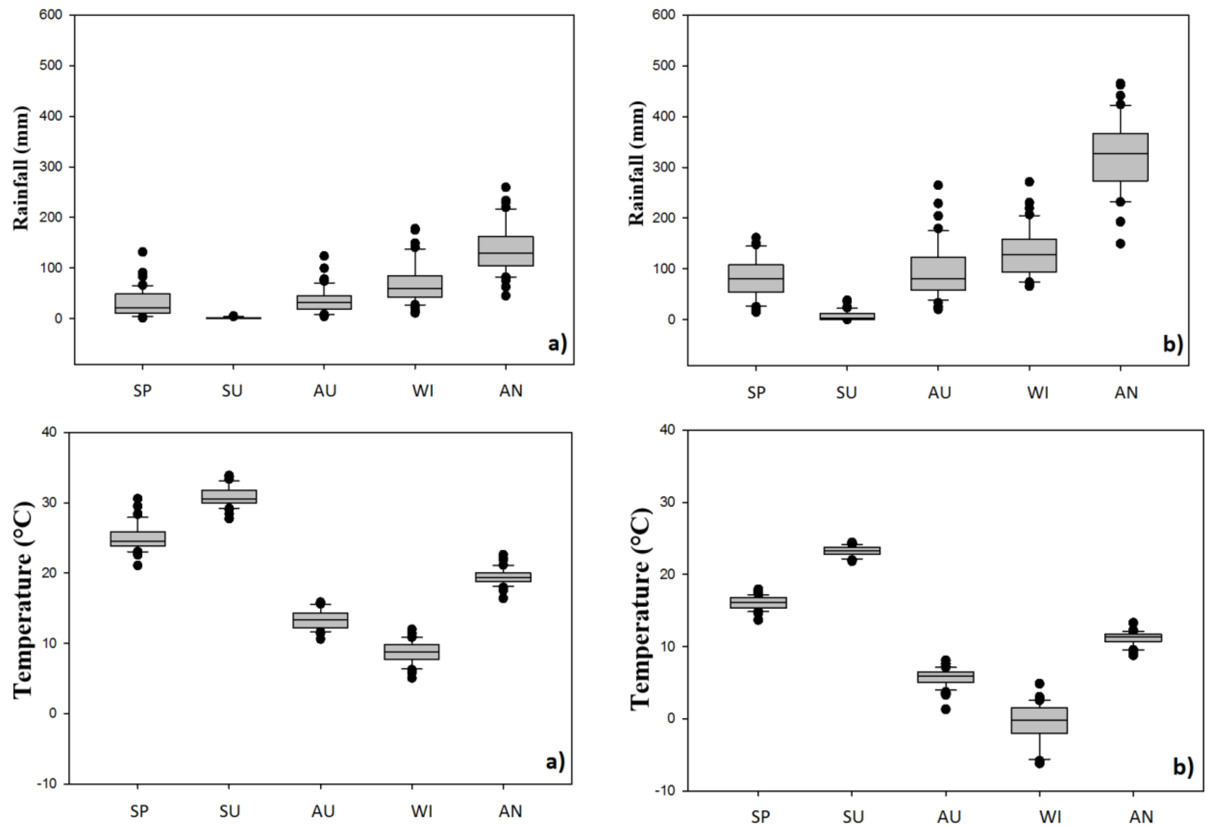

Fig. 3. Boxplots of rainfall and temperature during the period 1970-2015 in the selected stations, including (a) Kashan (south-east), (b) Hamadan (west). In boxplots, the first and third quartiles are indicated at the box's ends. Additionally, the horizontal line in the center of the box indicates the variable's median value. Vertical lines denote the variables' minimum and maximum values, whereas dots denote outliers. Time scales are defined: SP (Spring), SU (Summer), AU (Autumn), WI (Winter), AN (Annual). Please see Appendix (A) for other stations, including (c) Ghazvin (north-west), (d) Arak (south-west), (e) Tehran (north-east)

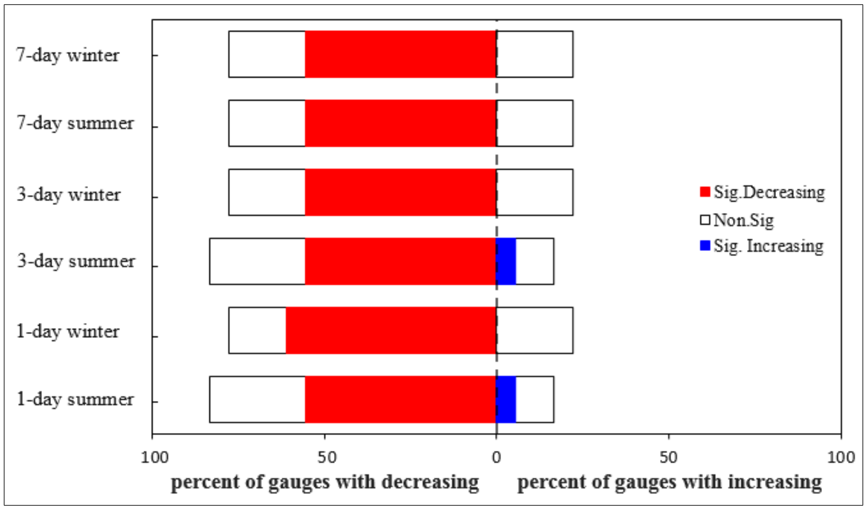

Fig. 4. Summary results of the spatial trend based on MMK test for seasonal low streamflows (1, 3, 7 days summer/winter low streamflow) in the Namak Lake basin (during 1970-2015)

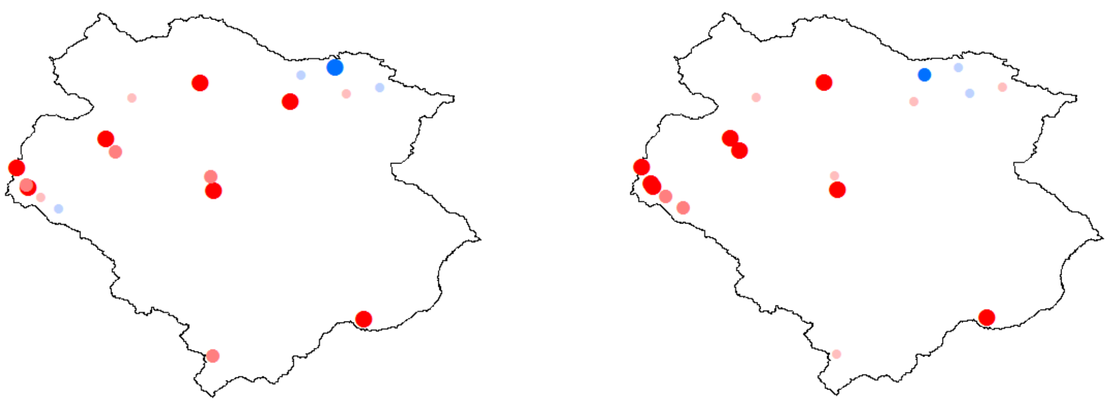

a) 1- day winter low streamflow

d) 1- day summer low streamflow

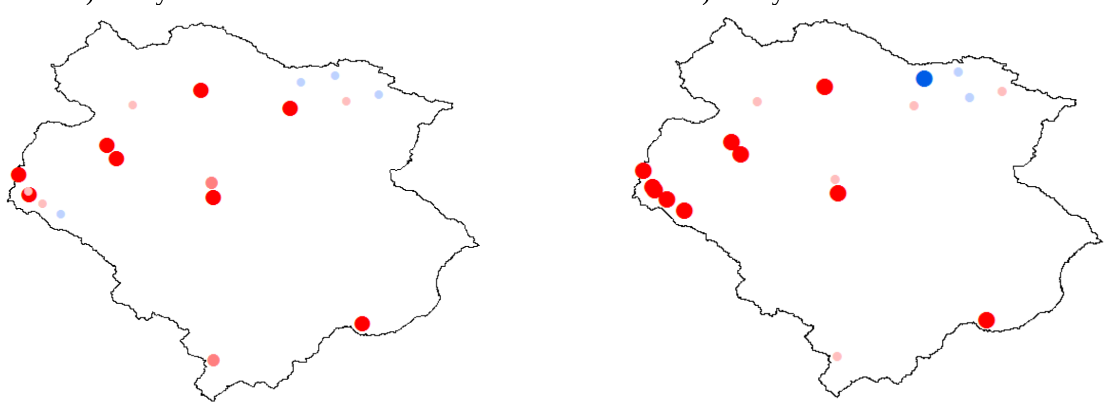

b) 3-day winter low streamflow

e) 3-day summer low streamflow

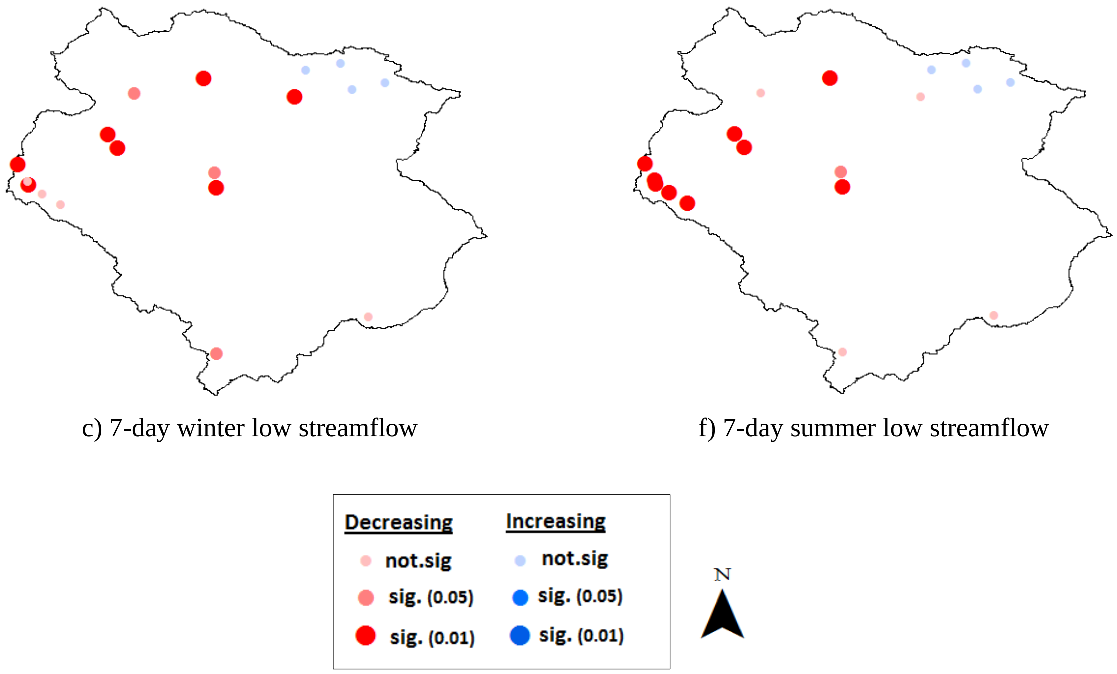

Fig. 5. The spatial distribution of long-term variations of 1, 3, and 7-days summer/winter low streamflows based on MMK test during the period of 1970-2015 in the Namak Lake Basin (size of the circles in the map indicates the significance level of the MMK test)

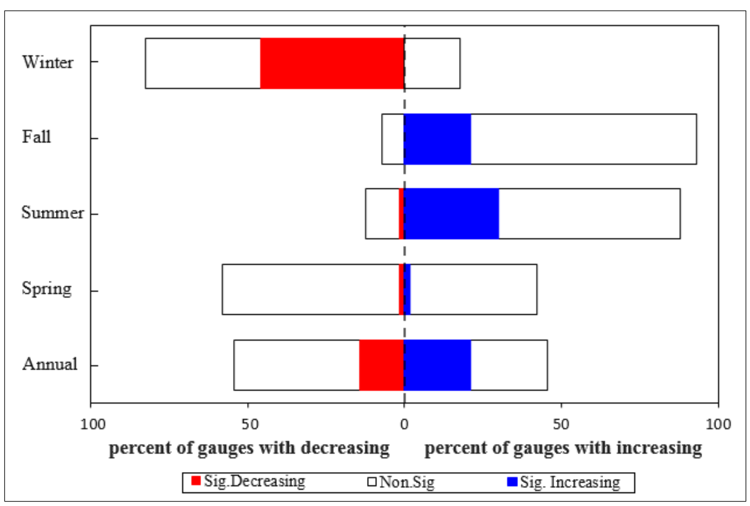

Fig. 6. Summary of long-term changes in seasonal and annual rainfall series based on the MMK test for the Namak Lake basin from 1970 to 2015

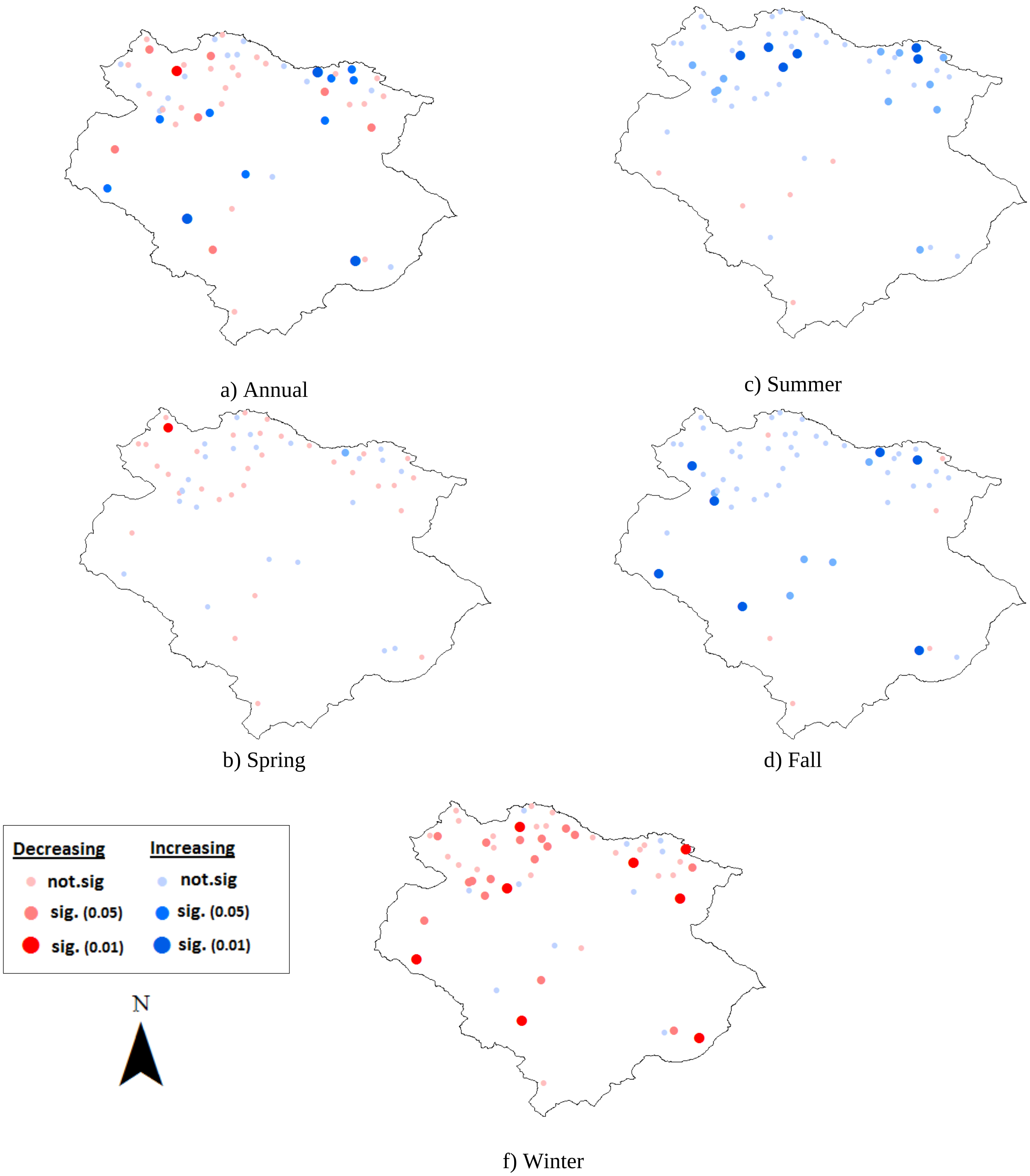

Fig. 7. The spatial distribution of long-term variations of seasonal and annual rainfall series based on MMK test during the period of 1970-2015 in the Namak Lake Basin (size of the circles in the map indicates the significance level of the MMK test)

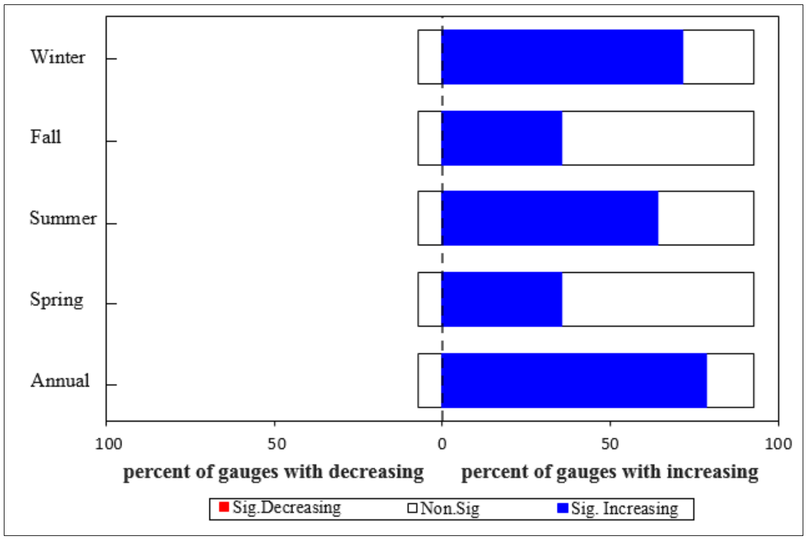

Fig. 8. Summary results of the spatial trend based on MMK test for seasonal and annual temperature series in the Namak Lake basin (during 1970-2015)

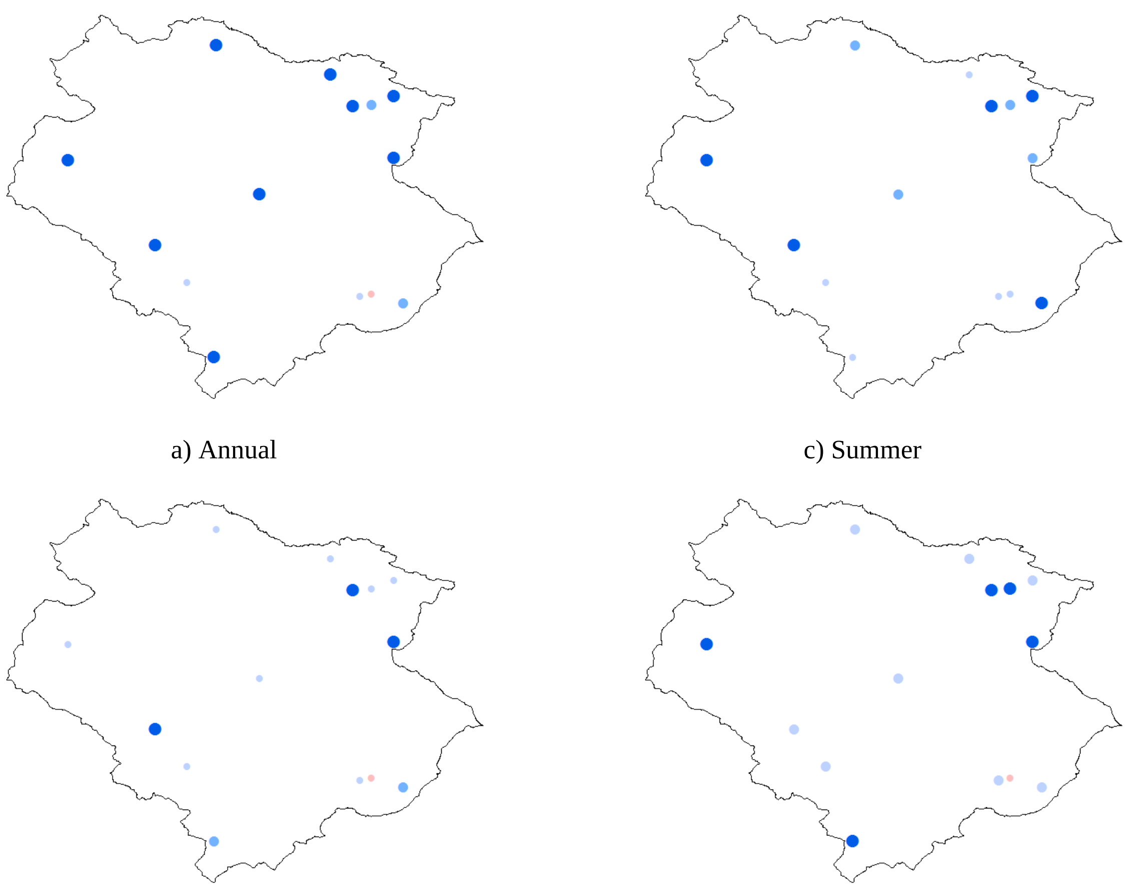

a) Annual

c) Summer

b) Spring

d) Fall

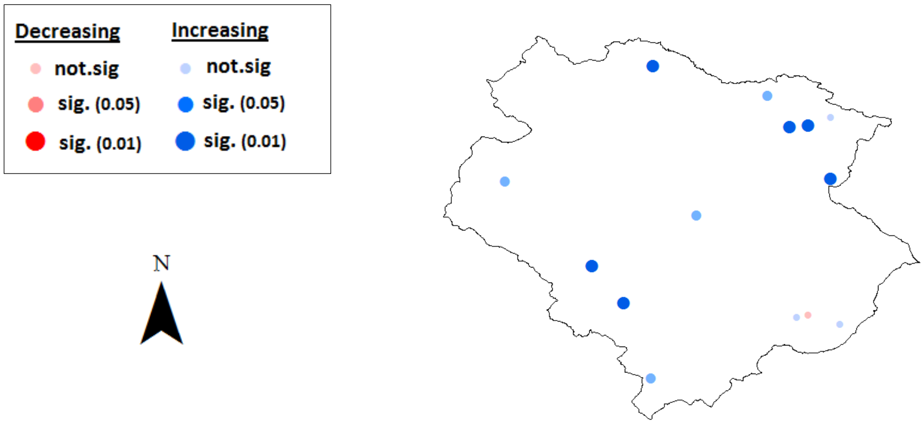

f) Winter

Fig. 9. The spatial distribution of long-term variations seasonal and annual temperature series based on MMK test during 1970-2015 in the Namak Lake Basin (size of the circles in the map indicates the significance level of the MMK test)

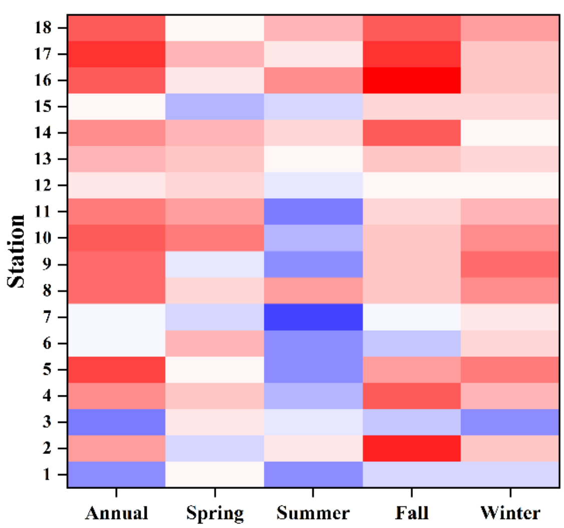

a) 1-day winter low streamflows

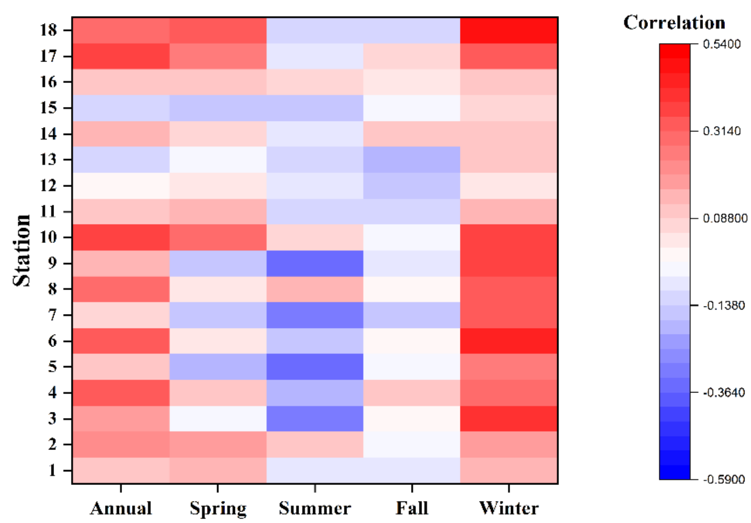

d) 1-day summer low streamflows

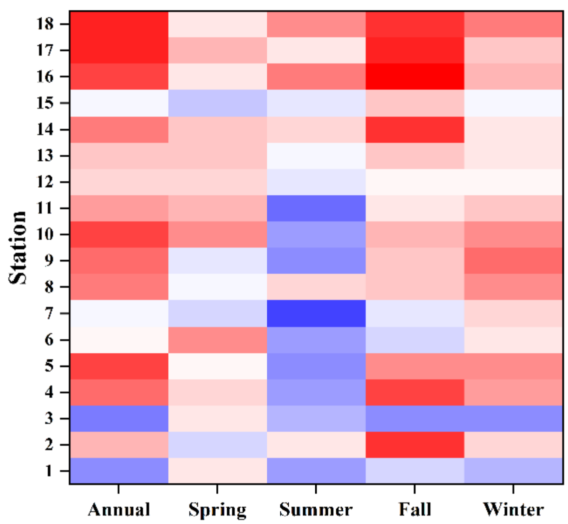

b) 3-day winter low streamflows

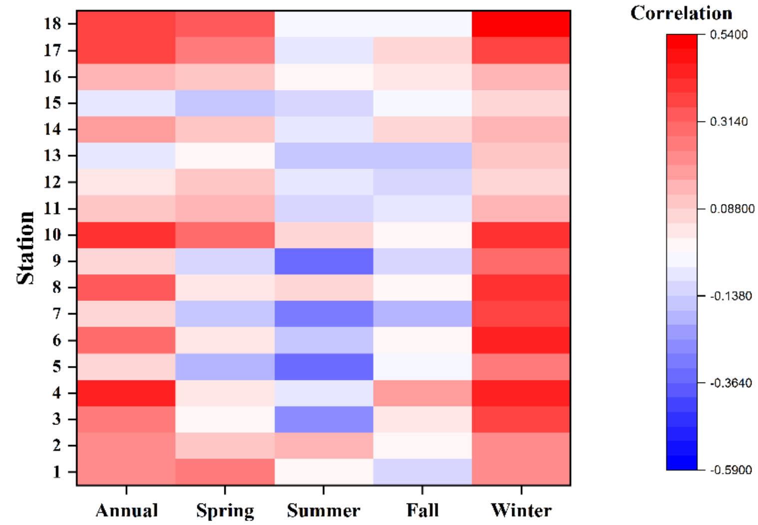

e) 3-day summer low streamflows

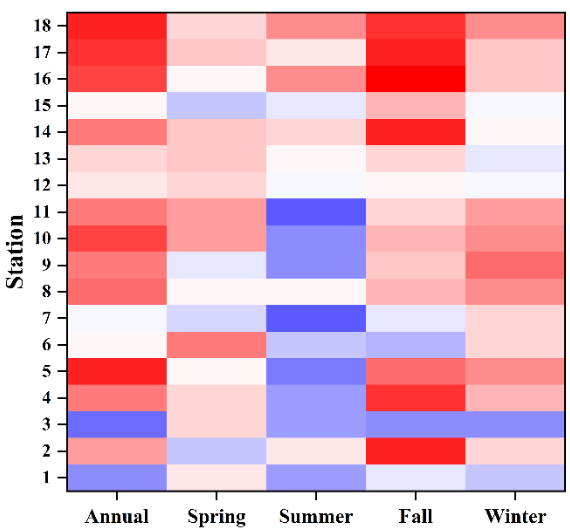

c) 7-day winter low streamflows

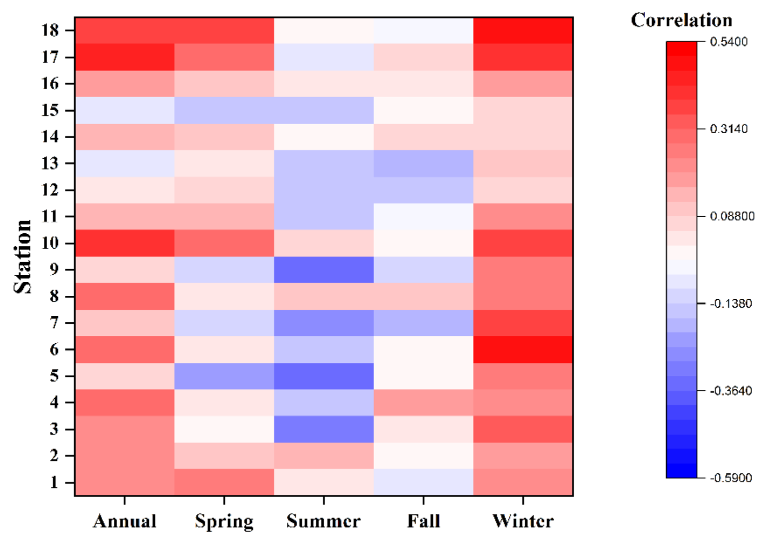

f) 7-day summer low streamflows

Fig. 10. The graphical results of the correlations between seasonal rainfall and low streamflows series based on the Spearman correlation coefficients during the period of 1970-2015 in the Namak Lake Basin (in the vertical axis, the stations number is based on Table 1)

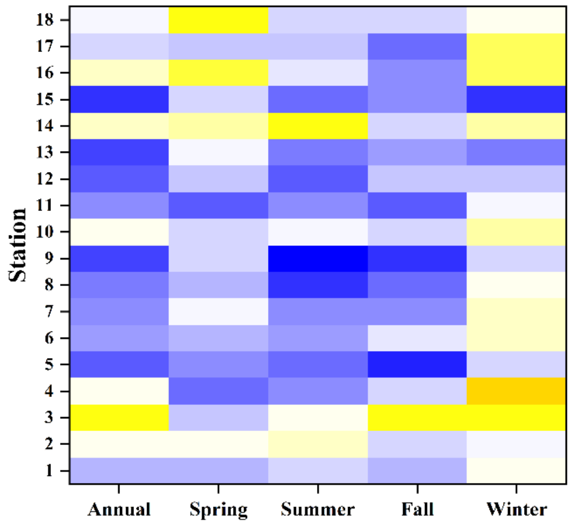

a) 1-day winter low streamflows

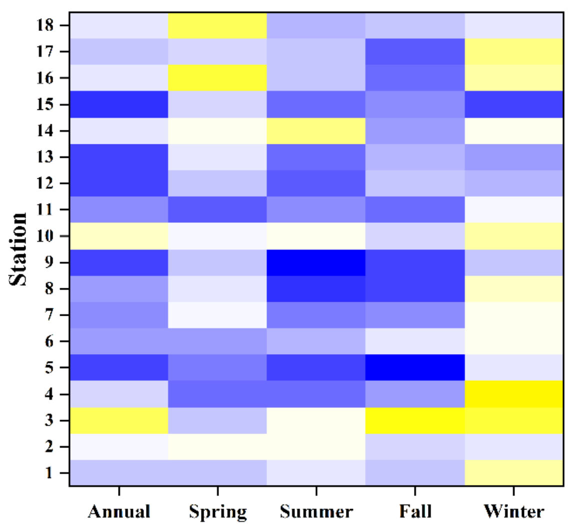

b) 3-day winter low streamflows

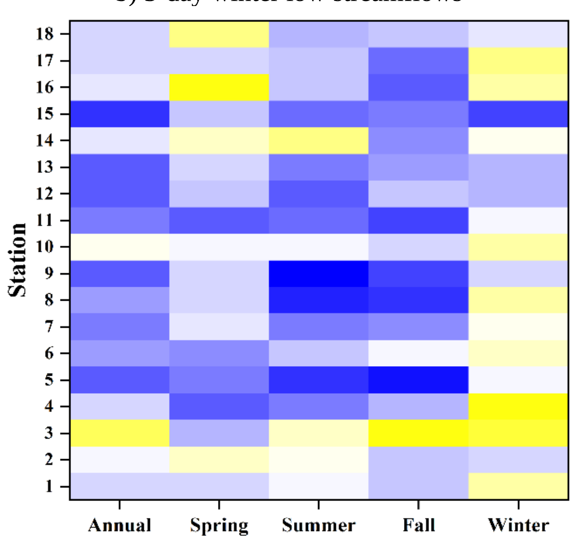

c) 7-day winter low streamflows

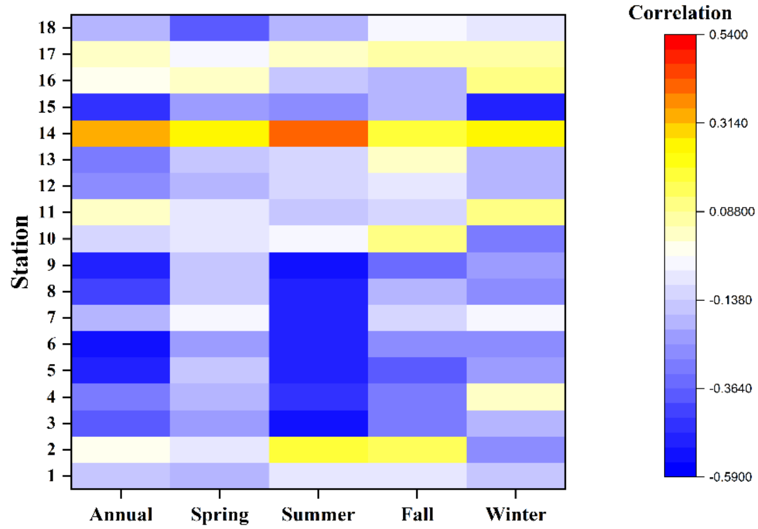

d) 1-day summer low streamflows

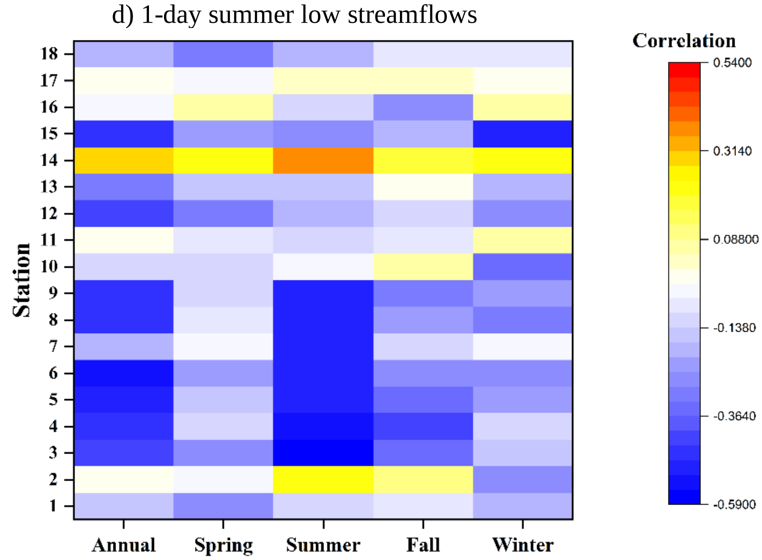

e) 3-day summer low streamflows

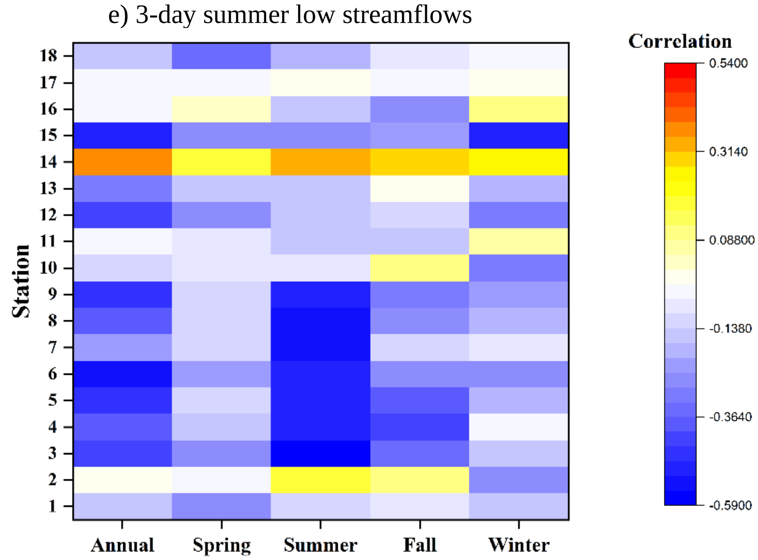

f) 7-day summer low streamflows

Fig. 11. The graphical results of the association between seasonal temperature and low steamflow series based on the Spearman correlation coefficients during the period of 1970-2015 (the station number is based on Table 1) in the Namak Lake Basin

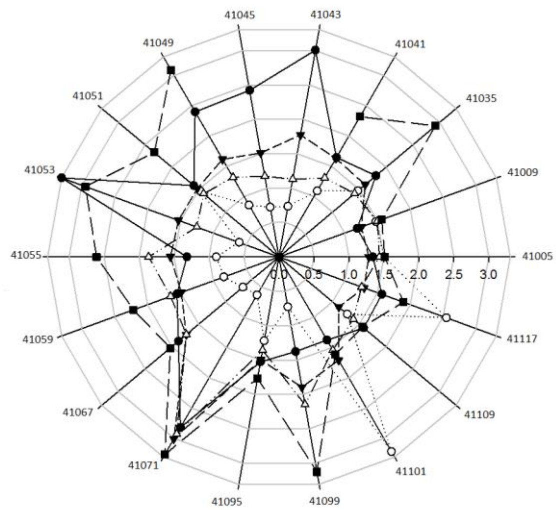

a) 1-day winter low streamflows

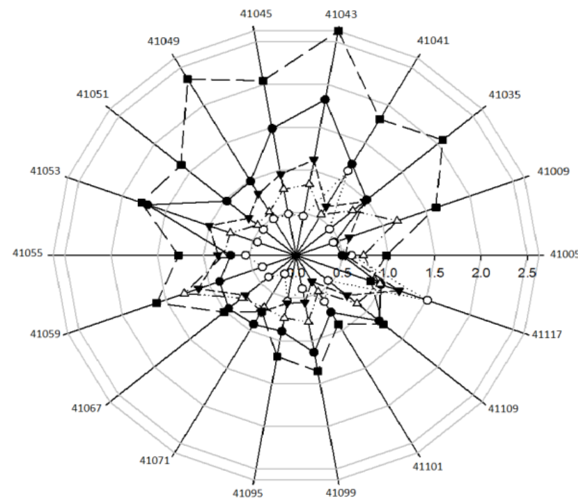

d) 1-day summer low streamflows

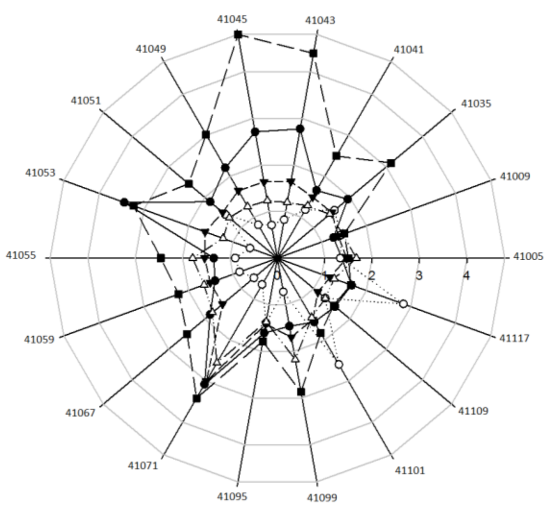

b) 3-day winter low streamflows

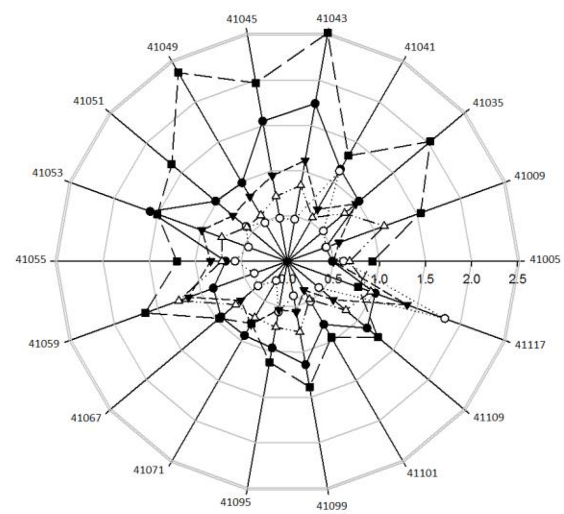

e) 3-day summer low streamflows

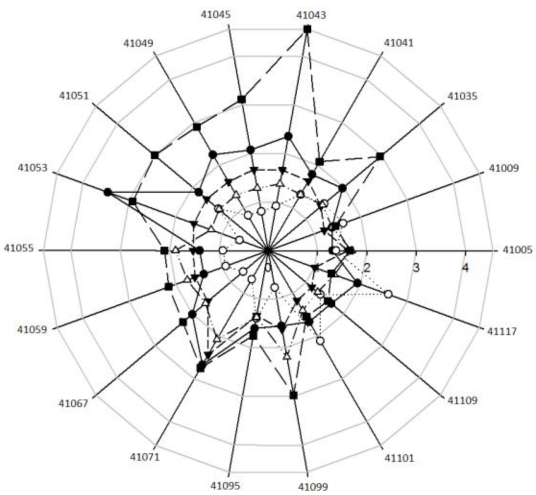

c) 7-day winter low streamflows

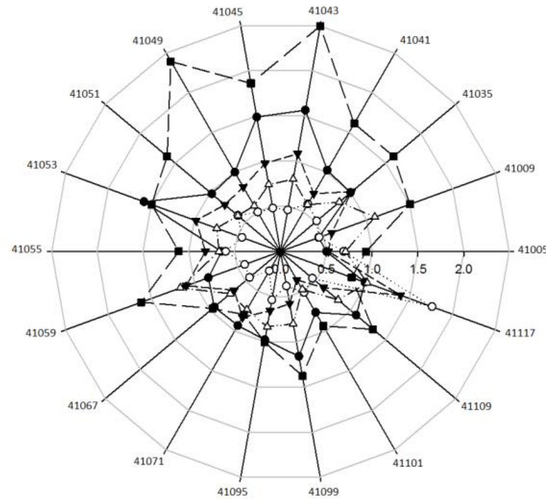

f) 7-day summer low streamflows

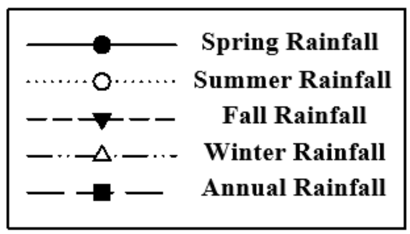

Fig. 12. Results of Cross-SampEn based on seasonal rainfall and low streamflow series at 18 hydrometric stations (the codes of the stations are based on Table 1)

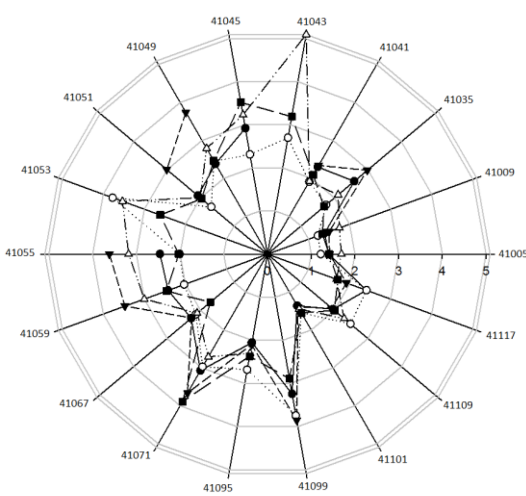

a) 1-day winter low streamflows

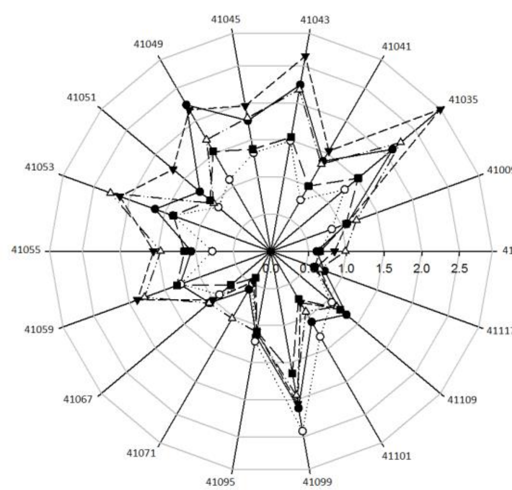

d) 1-day summer low streamflows

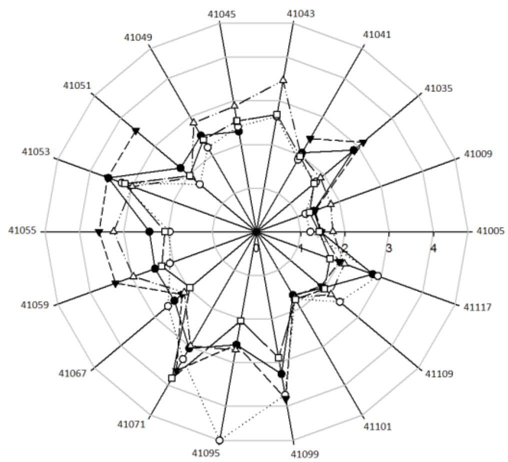

b) 3-day winter low streamflows

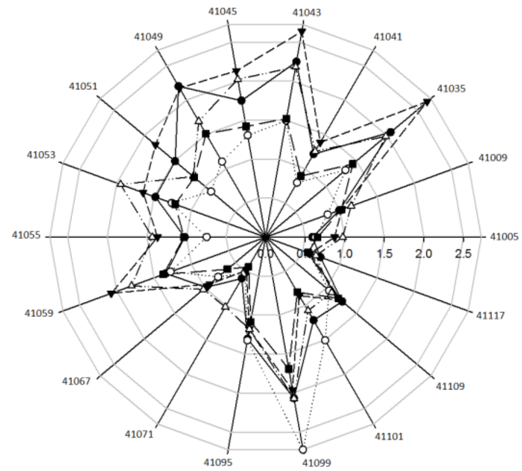

e) 3-day summer low streamflows

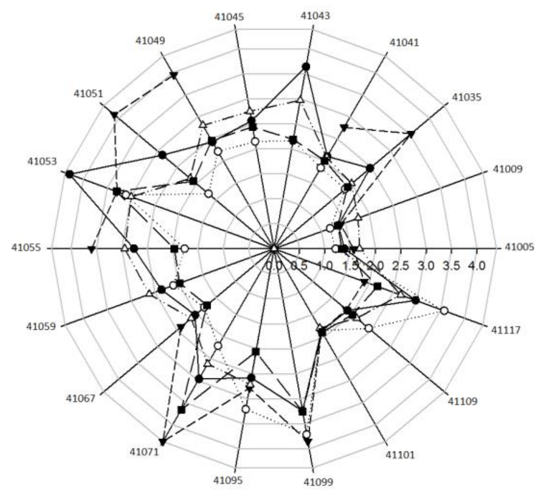

c) 7-day winter low streamflows

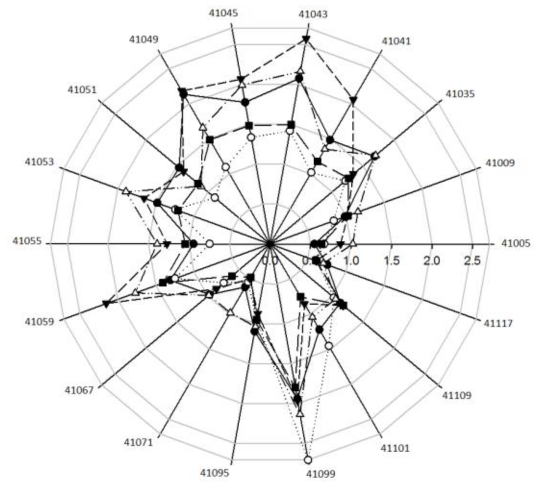

f) 7-day summer low streamflows

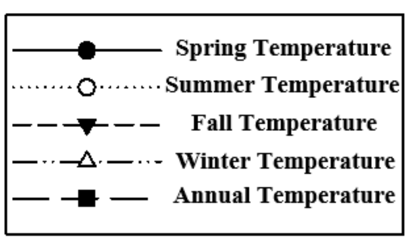

Fig. 13. Results of Cross-SampEn based on seasonal temperature and low streamflows time series at 18 hydrometric stations (the codes of the stations are based on Table 1)

Appendix (A)

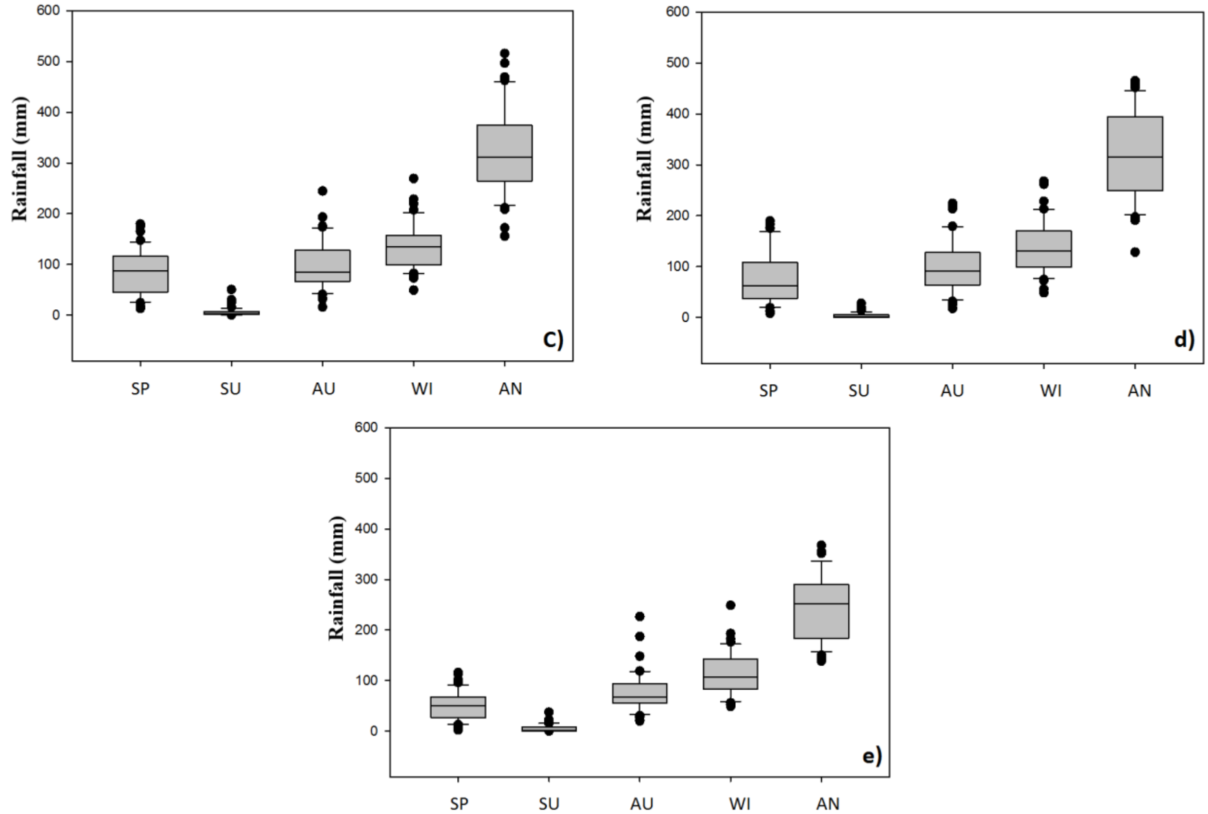

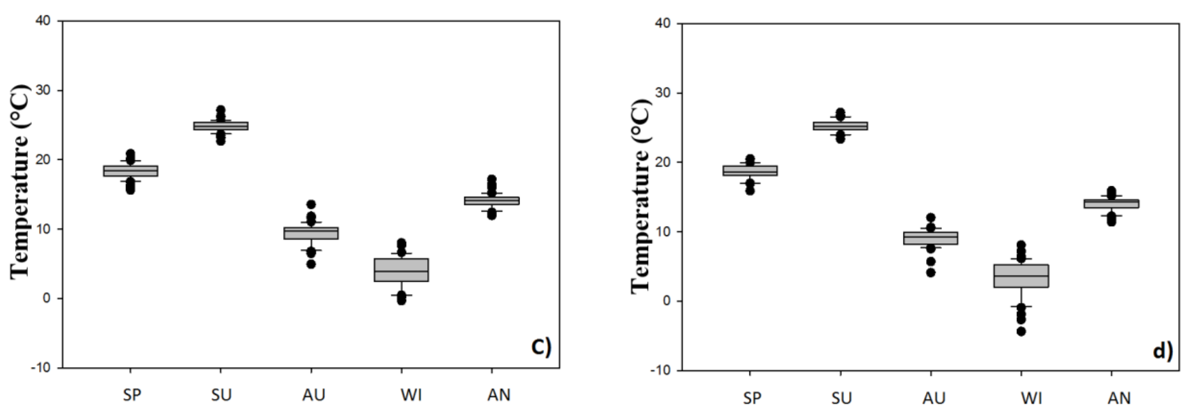

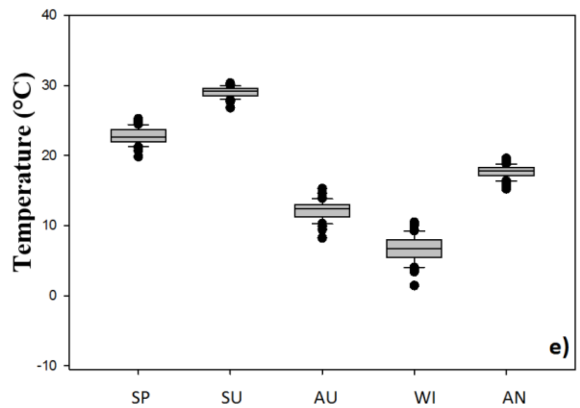

Fig. 3. Boxplots of rainfall and temperature during period 1970-2015 in the selected stations including: (c) Ghazvin (north-west), (d) Arak (south-west), (e) Tehran (north-east). Time scales are defined: SP (Spring), SU (Summer), AU (Autumn), WI (Winter), AN (Annual)

Appendix (B)

The first step to estimate Cross-SampEn measure is to normalize the two time series. For this purpose, each of the time series is subtracted from its mean, and divided by its standard deviation (SD). Therefore, two time series are obtained with zero mean and unit SD.

Mathematically, a review of the Cross-SampEn method is given below:

$$u = \left(u(1), u(2), ..., u(N)\right) \quad (1)$$

$$v = \left(v(1), v(2), ..., v(N)\right) \quad (2)$$

where u and v are two time series of length N. Two fixed input parameters m and r denote embedding dimension and the tolerance for accepting matches, respectively.

Form vector sequences

$$x_m(i) = \left(u(i), u(i+1), ..., u(i+m-1)\right), \; 1 \le i \le N-m \quad (3)$$

$$y_m(j) = \left(v(j), v(j+1), ..., v(j+m-1)\right) \; 1 \le j \le N-m \quad (4)$$

from *u* and *v*, respectively.

For each $i \le N - m$, set

$$B_i^m(r)(v \| u) = (\textit{number of } 1 \le j \le N - m \textit{ such that } d\left[x_m(i), y_m(j)\right] \le r)/(N - m) \quad (5)$$

where

$$d\left[x_m(i), y_m(j)\right] = \max\left\{\left|u(i+k) - v(j+k)\right| : 0 \le k \le m-1\right\} \quad (6)$$

i.e., the maximum difference in their respective scalar components. $B_i^m(r)(v \| u)$ is the probability that any $y_m(j)$ is within *r* of $x_m(i)$. And then define:

$$B^m(r)(v \| u) = \frac{\sum_{i=1}^{N-m} B_i^m(r)(v \| u)}{N - m} \quad (7)$$

which is the mean value of $B_i^m(r)(v \| u)$

Similarly, the following equations are defined:

$$A_i^m(r)(v \| u) = (\textit{number of } 1 \le j \le N - m \textit{ such that } d\left[x_{m+1}(i), y_{m+1}(j)\right] \le r)/(N - m) \quad (8)$$

and

$$A^m(r)(v \| u) = \frac{\sum_{i=1}^{N-m} A_i^m(r)(v \| u)}{N - m} \quad (9)$$

which is the mean value $A_i^m(r)(v \| u)$.

In this way, $B_i^m(r)(v \| u)$ is the probability that the two templates matches for *m* points, and $A_i^m(r)(v \| u)$ is the probability that the two templates matches for *m+1* points.

Finally, Cross-SampEn is defined as below:

$$Cross - SampEn = -\ln \left\{ \frac{A^m(r)(v \| u)}{B^m(r)(v \| u)} \right\}. \quad (10)$$

In this study, Cross-SampEn is estimated with *m=1* and *r=0.2*. The selection of parameters for *m* and *r* depends on the confidence interval for SampEn to Cross-SampEn.

A good SampEn should meet the following criterion defined by Lake et al. 2002:

$$r \geq \max(\sigma cp / CP, \sigma cp / -\log(CP)CP) \quad (11)$$

where *CP* is the conditional probability of length *m+1* given that there is a match of length *m*. This criterion is equal to the following condition:

$$95\%CI = -log\left(CP\right) \pm 1.96(\sigma cp / CP) \quad (12)$$

where 95%CI means a 95% confidence interval of the cross-SampEn that assumed to be normally distributed.

The calculation of Cross-SampEn requires three parameters including *N*, *m*, and *r*. *N*, *m*, and *r* indicate length of time series, length of vector being compared and the tolerance for admitting matches, respectively. Based on this method, as well as the choice *m*=1 and *r*=0.2 that *r* is an agreement to Richman and Moorman (2000) and Liu et al. 2010 (Richman & Moorman 2000, Liu et al. 2010). The only difference was observed in selecting *m*, due to the short length of signal *m=1* was considered.